GEOMETRY AND KINEMATICS OF THE YAKATAGA ANTICLINE, ICY BAY, ALASKA

By

Michael Scott Broadwell

RECOMMENDED:

Dr. Cathy Hanks

Dr. Paul McCarthy

Dr. Wes Wallace, Advisory Committee Chair

Dr. Paul Layer, Department Head,
Department of Geology and Geophysics

APPROVED:

Dr. David M. Woodall, Dean of the College of Science, Engineering, and Mathematics

Dr. Joseph R. Kan Dean of the Graduate School

9-21-01

Date

GEOMETRY AND KINEMATICS OF THE YAKATAGA ANTICLINE, ICY BAY, ALASKA

A

THESIS

Presented to the Faculty

of the University of Alaska Fairbanks

in Partial Fulfillment of the Requirements

for the degree of

MASTER OF SCIENCE

By

Michael Scott Broadwell, B.S., B.A.

Fairbanks, Alaska

May 2001

Abstract

The Yakataga anticline is a well-exposed asymmetrical fold with a ramp tip beneath the forelimb. Unconformities in the backlimb and forelimb indicate that both limbs rotated during fold growth. The stratigraphic character and evidence for deformation before full lithification suggest non-parallel folding by distributed strain rather than flexural slip. These characteristics of the natural fold do not fit existing models for thrust-related folds and I suggest two models for the Yakataga anticline's growth: 1) the fold formed as a non-parallel detachment fold modified by fault-propagation folding in the forelimb; and 2) the fold formed as a rotating-limb fault-propagation fold. The first of these models seems to fit the natural fold better because: 1) this model accounts for the subsidiary fold in the forelimb; and 2) rotation of the backlimb in the fault-propagation fold model requires a fanning of the bedding, a feature not observed in the natural fold.

Table of Contents

List of Figures

Acknowledgments

Thanks to Dr. Wesley K. Wallace for guidance during this work, providing a number of the photos used for interpretation, and conceiving of the idea as a Master's project, and to Dr. Cathy Hanks and Dr. Paul McCarthy for their helpful comments on the numerous drafts of this work. Thanks too are due to Arco Alaska (and especially Bob Swenson for his role in securing scholarship funds), the Department of Geology and Geophysics, and the Graduate School at the University of Alaska Fairbanks for supporting my time at UAF. My field season was supported in part by grants from the Department of Geology and Geophysics at the University of Alaska Fairbanks, BP (Alaska), the Alaska Geological Society, and the Geophysical Society of Alaska.

Introduction

Unparalleled exposures of structures related to the collision of the Yakutat terrane with Alaska resulted from the rapid retreat of the Guyot and Yahtse glaciers over the past 100 years in Icy Bay, located along the Gulf of Alaska between Yakutat and Cordova (Figure 1). One of these is the Yakataga anticline, which crops out in the Karr and Guyot Hills in Icy Bay. The extensive exposures have provided an outstanding opportunity to study the geometry of a natural fold, develop models for its evolution, and compare these to current models of fold growth. Of particular interest are the well exposed unconformities that separate the backlimb of the fold into several distinct parts, each with gentler dips up section, providing a progressive record of fold formation and serving as kinematic indicators. In addition, the Yakataga anticline is a thrust-related fold, with a ramp exposed where it cuts up section beneath the fold's forelimb, offering the chance to study the relationship between fault and fold.

The results of this study are applicable to fold-and-thrust belts worldwide and provide a natural test of models currently applied to thrust-related folds in similar settings. Since it is unusual to find such dramatic exposures as those in Icy Bay, the interpretation of an area or structure is typically based largely on models. The specific model used has implications for the extrapolation of data into the subsurface and into areas where the data are incomplete, so it is important that the models be tested against natural folds. Such testing develops criteria that allow for the most appropriate model to

Prepared for submission to the Journal of Structural Geology: Pergamon, Oxford, International

be chosen when extrapolating folds into areas where the data are unavailable, such as the subsurface.

Statement of the Problem

The Yakataga anticline has been cited as an example of a specific type of thrust-related fold, a fault-propagation fold (Suppe and Medwedeff, 1990, figure 8). The backlimb channels in the outcrop, however, serve as prominent kinematic indicators that require rotation of the backlimb during fold growth. A rotating backlimb is inconsistent with fault-propagation fold models. This begs the question then, how did the Yakataga anticline form and how will a model of its development compare to current models for thrust-related folds?

Location and Geologic Setting

The area of this study includes the Yakataga anticline where it crops out in the western flank of the Karr Hills, located in Icy Bay adjacent to the Yahtse Glacier (Figure 1). The area is in Wrangell - St. Elias National Park, Township 20 S, Range 24 E in the Bering Glacier A-1 quadrangle.

Tectonic Setting

The Gulf of Alaska extends across a complex collisional zone between the Pacific and North American plates that forms a transition between subduction along the Aleutian trench and transform along strike-slip faults farther east, such as the Fairweather fault (Figure 1). This region has been the location of a complex history of plate interactions, causing the assembly of a number of distinct tectonostratigraphic terranes during the

Mesozoic and Cenozoic eras into the present continental margin (Plafker, 1987). The southernmost of these terranes is the Yakutat terrane, which is currently moving with the Pacific plate and colliding with North America (Bruns, 1983; Plafker, 1987).

The Yakutat terrane is bounded by the Fairweather fault to the east, the Chugach-St. Elias fault to the north, and the Kayak Island fault zone to the west (Figure 1) (Plafker, 1987). The Pacific plate is carrying the Yakutat terrane towards the northwest, resulting in strike-slip along the Fairweather transform and a large component of compression being taken up by folding and thrusting within the northern part of the Yakutat terrane (Plafker, 1987). In a general way, deformation is progressively younger toward the Pamplona zone (Figure 1), to the west of which lies a significant fold and thrust belt, and to the east of which lie relatively undeformed rocks in an aseismic zone (Bruns, 1983; Plafker, 1987). The Yakataga anticline lies just north of the Pamplona zone and formed relatively recently.

The Yakataga anticline is formed in the Yakataga Formation, a thick accumulation of marine and glacio-marine sediments that have been deposited from Late Miocene to the present (Eyles and Lagoe, 1998) (Figure 2). The Yakataga Formation represents an enormous volume of clastic detritus, characterized by a large amount of glacially derived material that was shed from the Chugach and St. Elias mountains and deposited on the continental margin. As a consequence of the continuing collision between the Yakutat terrane and Alaska, these sediments were rapidly deformed and uplifted, leaving a widely distributed accumulation of the Yakataga Formation onshore

that is up to 4600 m thick (Plafker, 1987). Offshore, the deposition of the Yakataga Formation continues today (Plafker, 1987).

The Yakataga Formation has been a focus of past research because of the impressive mega-channels preserved in the stratigraphy (Armentrout, 1983; Eyles and Lagoe, 1998). Recent interpretations of these submarine channels attribute their presence to large-scale slumping, triggered either by seismic activity or increasing instability on the flanks of a growing structural high (Eyles and Lagoe, 1998). The channels are of interest to this study because of the unconformities that resulted from syn-deformational channel formation. These unconformities separate the limbs of the Yakataga anticline into several domains that display progressively gentler dips up section, suggesting synchronous folding and deposition and leaving a continuous record of fold formation.

Based on oxygen isotopes, Eyles and Lagoe (1998) have dated deposition of the Yakataga Formation in Icy Bay as starting during the mid-Pliocene warm event (Early Pliocene). The mega-channels do not appear, however, until higher up section in rocks influenced by glaciation (Late Pliocene to Pleistocene) (Eyles and Lagoe, 1998) (Figure 2). While the age of the rocks in the Yakataga anticline itself cannot be determined based on the available data, they can be constrained to be younger than Late Pliocene to Pleistocene (about 2 ma) on the basis of this stratigraphic relationship.

Methods

In order to accomplish this study, I completed a 6-½ week field season during the summer of 1998. My original plan was to map in as much detail as possible, paying

particular attention to the well-exposed unconformities. What looked like passable terrain from topographic maps and air-photos, however, turned out to be a landscape dissected by deep and narrow canyons and replete with steep cliffs of rotten rock due to the recent deglaciation. As the realities of the topography took hold, the focus of this work shifted to the only accessible part of the fold, the footwall ramp, and time was spent documenting the geometry in this area. Interpretations of the rest of the structure are based on sketches, air photos (Appendix) and photos taken of the anticline while in the field. The photos are the main database from which I created a cross section of the structure. This cross section in turn provided a basis for balancing and testing several different models of fold evolution.

New fold models: All of the original models presented in this work were generated using the AutoCAD software package. They are all area balanced, but not necessarily line-length balanced. I chose 2-dimensional, simple kink-band geometries because of their relative ease of use and the well-established history of this approach (e.g., Suppe, 1983; Chester and Chester, 1990; Mitra, 1990; Suppe and Medwedeff, 1990; Mosar and Suppe, 1992; Epard and Groshong, 1995; Poblet and McClay, 1996; Homza and Wallace, 1997). Initial assumptions vary for each of the new models and are addressed individually.

Thrust-related fold models

A number of models exist that describe the kinematics of thrust-related folds, the most well known of which include fault-bend folds, fault-propagation folds, and

detachment folds. The Yakataga anticline has been cited as an example of a fault-propagation fold (Suppe and Medwedeff, 1990, figure 8). The standard models for fault-propagation folds attribute folding to be simultaneous with and a consequence of propagation of a fault up a ramp (Figure 3) (Mitra, 1990; Suppe and Medwedeff, 1990). Slip along the fault decreases up section and is accommodated by fold formation. The model predicts a geometry that includes steeply dipping to over-turned forelimbs and a backlimb dip that is constant and related to the dip of the ramp. Some models have been proposed that allow for rotating forelimbs, generally as a result of a shear gradient, but even in these cases the backlimb dip is either fixed by the ramp and remains unchanged as the fold grows (Mitra, 1990; Mosar and Suppe, 1992) or the backlimb is simply not addressed at all (Erslev, 1991).

Some models for detachment folds do, however, call for limb rotation (Figure 4) (Homza and Wallace, 1995; 1997; Poblet and others, 1997). Of the current well-known thrust-related fold models, only detachment folds allow for rotation of both forelimbs and backlimbs. Detachment folds form due to the structural thickening of an incompetent unit, typically beneath a more competent unit and above a bed-parallel thrust, and can result in a wide range of possible geometries.

Most of the models cited above were formulated using the concepts of cross section balancing (De Paor, 1988), the end results of which were geometric/mathematical models of folds. When presented in steps showing the development of the fold at different stages the models illustrate the kinematics of fold development (Figures 3 and 4). The kinematics can often be purely hypothetical, although the use of strain indicators

like fractures, cleavage, and extension veins is a common tool to constrain actual deformation pathways. For example, the location of such indicators can shed light as to whether hinges were fixed or migrated during fold growth (e.g., Homza and Wallace, 1995).

Mechanical Stratigraphy

The role of mechanical stratigraphy in the formation of structures has been recognized for some time (e.g., Woodward and Rutherford, 1989; Fischer and Jackson, 1999). Among their other seven main controls on fold geometry, Ramsay and Huber (1987, p. 405) included "The mechanical properties of the interfaces between layers" and "The thickness of each of the constituent layers in the rock packet, and whether or not the different rock layers are grouped into units." Commonly, no explicit statements about the role of mechanical stratigraphy are included in discussions of the origins of structures, although implicit assumptions regarding the mechanical stratigraphy, whether appropriate or not, are usually built in. When the influence of mechanical stratigraphy on a structure or region is discussed, it is generally assumed that a contrast in competencies between distinct mechanical units influenced the style of deformation. Studies relating competency contrasts in the mechanical stratigraphy to the resulting map-scale structures can be readily found in the literature (e.g., Pfiffner, 1993; Davis and Lillie, 1994), but discussions regarding the role of mechanically weak and homogeneous successions of sediment on the geometry and evolution of map-scale structures are seemingly rare.

Treatments of detachment folds should take the stratigraphy into account pretty

much by definition, as detachment folds are generally assumed to form by competent beds folding above a weaker unit in the core (Poblet and McClay, 1996; Homza and Wallace, 1997). Fault-propagation folds, on the other hand, are generally presented with no acknowledgement of the stratigraphy at all. The model is applied uniformly to any succession of rocks. Implicit in standard fault-propagation fold models, however, is the assumption of layer-parallel slip (Mitra, 1990; Suppe and Medwedeff, 1990), the likelihood of which is going to be dependent on the availability of surfaces on which slip can occur. This is not a valid assumption for all stratigraphic sequences. Layer-parallel slip can be expected to have little influence in successions that are mechanically uniform, lacking in mechanically defined bed surfaces, and generally weak.

Geometry of the Yakataga Anticline

The Yakataga anticline is an asymmetric, east-northeast-trending anticline that plunges gently (Figure 5) and has a steeply dipping to overturned forelimb (Figures 6 and 7). In natural thrust-related folds, the fault itself is rarely seen and must be inferred, usually based on a chosen model. In the Yakataga anticline, a ramp is exposed and, even more unusual, we were able to locate the ramp tip (Figure 8). The beds in the footwall are sub-horizontal and undeformed. A back-thrust is obvious above the ramp tip cutting through the distinct, striped beds (Figure 8). A strongly fractured zone that likely represents localized normal faulting (or potentially tension fractures) in the footwall and thrusting or shear fracturing in the hangingwall (Figure 9) characterizes the area around the fault tip. The lack of distinctive bedding to serve as structural markers makes it hard

to judge the true nature of the fracturing, but a similar fracture geometry has been observed around fault tips elsewhere to accommodate displacement reduction by extension in the footwall and contraction in the hangingwall (Hyett, 1990).

In terms of scale, the exposed folded beds stretch 1.5 miles (2.4 kilometers) along the Yahtse glacier fjord and reach an elevation of 4000 feet (1220 meters) above sea level. The majority of the backlimb dips at 34 degrees. Beds in the forelimb are much harder to characterize, and are also stratigraphically more variable. They range from sub-vertical to overturned and dipping 51 degrees (as determined by field measurements). The dip on the exposed portion of the ramp is 15 degrees.

Large-scale mega-channels are visible in both the forelimb and the backlimb (Figures 6 and 10). The differences in dip across the channel unconformities are particularly obvious in the backlimb (Figure 11). There are two primary channels in the backlimb, the first of which has beds dipping at 22 degrees, and the second of which truncates the top of the entire Yakataga anticline and contains beds that are sub-horizontal. Channel geometries in the forelimb are much more difficult to interpret because bedding dips steeply and is completely dissected by channel unconformities (Figures 12 and 13). There is, however, a prominent angular unconformity that can be traced to a point just below the hinge (Figure 14). In part of the forelimb, the beds overlying the unconformity are conformable with the unconformity surface, which truncates the underlying beds. However, there is some ambiguity in this interpretation elsewhere, and it is likely that the geometry of the unconformity surface is changes

depending on its position in the fold, with the overlying beds in places lying conformably over and in others onlapping the surface.

A number of smaller, meso-scale structures such as folds and faults are visible in the accessible region of the fault tip, some of which present their own curious geometric problems (Figure 15). It is not entirely clear if these small structures represent tectonic or depositional deformation, but Eyles and Lagoe (1998) have documented similar structures beneath channel contacts and interpreted their formation to be related to channel deposition. If the channels formed syn-deformationally, it follows that the rocks of the Yakataga Formation were not well lithified at the time of folding.

Mechanical Stratigraphy of the Yakataga Formation

The rocks forming the Yakataga anticline are interbedded sandstones and diamictites of the Yakataga Formation, a thick, mechanically homogeneous sequence of marine and glacio-marine sediments (Eyles and Lagoe, 1998). The stratigraphy of this area has been the focus of past work by Eyles and others (1991) and Eyles and Lagoe (1998) and two of their sedimentological logs are included here (Figures 16 and 17). A section measured in the basal part of the Icy Bay succession near the mouth of the bay (Figure 16) is much lower in the stratigraphic column than the rocks exposed in the Yakataga anticline in the Karr Hills, although it is difficult to guess just how much lower it is in the section. This section differs from the stratigraphically higher sections presented here (Figures 17 and 18) in that it appears to offer greater possibility for mechanical contrasts, better lending itself to potential detachments beneath the strata

exposed at the Yakataga anticline. This becomes important, as all the models presented below assume a detachment at depth. A section measured by Eyles and Lagoe (1998) higher in the succession (Figure 17) is in the rocks that make up the Yakataga anticline. This section was measured within the Yahtse channel, the name Eyles and Lagoe (1998) gave the prominent backlimb channel in the Yakataga anticline where it is exposed in the Guyot Hills.

The part of the Yakataga Formation represented by Figure 17 consists of thick layers of relatively homogeneous and mechanically isotropic rocks. My own measured section of the part of the Yakataga Formation that is visible and accessible near the ramp (Figure 18) also shows a succession of relatively homogeneous lithologies. The changes between some units are hard to define and there are no obvious mechanical discontinuities between beds to serve as flexural slip surfaces. In Icy Bay, we find a thick sequence of indistinct units, the differences between which are commonly subtle. This is in sharp contrast with the sort of succession in which many map-scale folds have been described, such as a clear succession of interbedded limestones and shales with clean bedding surfaces, distinct competency differences, and ample opportunity for flexural slip (e.g. the Brooks Range in Alaska, Homza and Wallace, 1995; 1997). In the Yakataga anticline, bedding surfaces are irregular and separate units of similar lithologies. Any slip surfaces that may be present would be discontinuous at best, as the entire sequence has been dissected by large-scale channels, making it difficult to trace any beds for more than a short distance (Figure 12).

In addition, these rocks were not well lithified at the time of deformation as suggested by their young age and indicated by the impressive soft-sediment deformation (Figure 19). In places the timing of the soft-sediment deformation can be said to have occurred simultaneously with structural deformation, as the soft-sediment deformation has occurred along the margins and as a result of channel formation (Eyles and Lagoe, 1998). Since the channels themselves are syn-deformational, this indicates that the Yakataga Formation was still wet and mechanically weak at the time of fold formation.

Discussion of mechanical stratigraphy: All of the above has implications for the mechanical behavior of the sediments. Instead of conceptualizing a rigid beam deforming above a ductile medium as with most detachment fold models, or a series of beams slipping past one another as they fold above a propagating ramp tip as with the fault-propagation fold models, the Yakataga Formation probably deformed most readily by internal strain and may have acted something like a salad made up of alternating layers of gelatin.

Epard and Groshong (1995) proposed a model for detachment folding that essentially treats the stratigraphy as mechanically homogeneous and isotropic (Figure 20). They defined detachment folds as "a general geometric concept for any fold formed above a stratigraphically fixed detachment horizon and that does not have displacement transferred out of the structure on an upper detachment" (Epard and Groshong, 1995, p.85). No mention is made of either a competent layer deforming above an incompetent layer, nor of the necessity of layer-parallel slip. In fact, no mention of stratigraphy is made at all. In essence, their model describes deformation of a single, mechanically

homogeneous layer with a few mechanically passive marker beds included to define the fold. The Epard and Groshong model requires internal strain to accommodate folding while maintaining area balance, and they suggest this strain can be taken up by various mechanisms that are homogeneous at the scale of the fold, including penetrative strain, second-order folding, second-order faulting, or a combination of these (Figure 21). Epard and Groshong go on to suggest that penetrative homogeneous strain is unlikely in low-temperature deformation. That may be true for well-indurated rocks, but I do not think that penetrative homogeneous strain can be ruled out for the Yakataga Formation, which was deformed when it was young, wet, and weakly lithified. It is difficult, however, to document penetrative homogeneous strain in the rocks of the Yakataga anticline because most of the fold is inaccessible due to the severity of the topography. Other features, like second-order folding, are obvious in rocks surrounding the ramp tip (Figure 15).

The stratigraphic assumptions built into the Epard and Groshong model approximate the conditions interpreted to exist in the Yakataga Formation at the time of folding. The model allows for rotating limbs and is applicable to a wide range of possible geometries. Consequently, it serves as a good starting point for further modeling.

Importance of the backlimb channels

Many of the beds in both the forelimb and the backlimb of the Yakataga anticline are concordant across channel surfaces, but where discordance does exist across a

channel unconformity this documents syn-deformational deposition in both limbs and puts constraints on possible deformation paths. Discordance in the backlimb is obvious (Figures 6, 10, and 11) and there is at least one angular unconformity in the forelimb (Figure 12 and 14). Both limbs are required to rotate in order to form this pattern of changing limb dips (Figure 22) (Poblet and Hardy, 1995; Zapata and Allmendinger, 1996; Ford and others, 1997; Poblet and others, 1997; Poblet and others, 1998). Because of this, the dip changes across channel unconformities serve as the primary kinematic indicator used to constrain later modeling of the Yakataga anticline. To successfully model the formation of the Yakataga anticline, any model will have to account for rotation of both limbs.

It is hard to trace the stratigraphically highest unconformity, above which the beds are sub-horizontal in the backlimb of the fold, across the anticline hinge and into the forelimb because of erosion and complex topography (Figures 6, 10, and 12). Two possibilities are: 1) the unconformity predates the latest folding and is itself folded; or 2) the unconformity post-dates most of the folding and the beds are unaffected where they cross the anticline. While I cannot reliably correlate beds or unconformities across the hinge, it seems likely that the angular unconformity in the forelimb is a continuation of the uppermost unconformity seen in the backlimb (Figure 12). With the beds overlying the unconformity in the forelimb interpreted to be conformable to the unconformity surface, the unconformity must pre-date the latest folding.

Models for the Yakataga anticline

The final geometry of the Yakataga anticline is certainly consistent with theoretical fault-propagation fold models. Notably, fault-propagation models are the most widely recognized of the current thrust-related fold models that involve a ramp tip. However, "Final geometry does not necessitate a particular deformation history" (Passchier and others, 1992) (Figure 23), and this alone cannot be used to conclusively classify the Yakataga anticline as a fault-propagation fold. A significant deviation of the Yakataga anticline from fault-propagation fold models is the strong evidence of backlimb rotation. The growth strata seen in the channel deposits provide a clear record of increasing backlimb dip during fold growth, a characteristic not predicted, nor allowed, by fault-propagation fold models. As previously mentioned, some fault-propagation fold models have been proposed that do allow for rotating forelimbs (Mitra, 1990; Erslev, 1991; Mosar and Suppe, 1992), but even in these cases the backlimb dip is fixed by the ramp and remains unchanged as the fold grows.

The geometry of the natural Yakataga anticline is also consistent with theoretical detachment fold models in many ways (although hardly unique to detachment folds). The key similarity is the evidence for rotation of both limbs. The ramp may have cut up section from a bed-parallel detachment in the subsurface. However, this deviates from a simple detachment model because detachment folds are defined as forming above bedding-parallel detachments, not ramps. Most detachment fold models also assume a stratigraphy that includes large differences in mechanical competency, which is not the case in Icy Bay.

As Suppe (1983, p.693) states about his model for fault-bend folding, "If a structure cannot be successfully described by these equations then either it is not a fault-bend fold, the assumptions are not valid, or the structure is too complicated to solve given the limited data available." The quote holds true if any other thrust-related fold model is substituted. I have described the similarities between the natural Yakataga anticline and the theoretical models for detachment folds and fault-propagation folds, but it is clear that neither detachment fold or fault-propagation fold models fully account for all of the characteristics of the natural structure. How then did the Yakataga anticline form? I have tried to answer that question by testing different geometric-kinematic models against the constraints provided by the Yakataga outcrop. Two possibilities were considered: 1) the Yakataga anticline formed initially as a detachment fold that was later cut by a ramp and modified by fault-propagation folding; and 2) the Yakataga anticline formed as a rotating-limb fault-propagation fold. These seem like the most likely possibilities, although other kinematic pathways surely are possible.

The purpose of these models is not to achieve a perfect representation of all facets of the natural geometry. Rather it is an attempt to observe the consequences of different model assumptions using approximations of the natural geometry. The end results are not unique and are not intended to be exact models of the Yakataga anticline. Further iterations could have refined the models to better match the actual geometry of the natural fold, but that was beyond the scope of this work.

1) Model A: Initial detachment fold later modified by fault-propagation folding

One possibility I tested was the idea that the Yakataga anticline began as a detachment fold that formed with rotating limbs above a bedding-parallel thrust. A ramp later cut up section, superimposing a fault-propagation fold geometry on the forelimb of the existing structure as the detachment fold was further displaced. This model is referred to as "model A."

The first step in this model is naturally the formation of an initial detachment fold. To build this early fold, I started with the geometry of a bed close to the core of the natural fold that was seemingly unaffected by structures possibly resulting from later propagation of the ramp tip (Figure 24). The geometry of this layer became the lowermost marker bed in all cross sections illustrating model A, and was assumed to represent the final stage of detachment fold development.

The geometry of the beds above this lowermost marker bed was built using the Epard and Groshong (1995) model (see "**Discussion of mechanical stratigraphy"** on page 19 for explanation), and depended entirely on the depth to detachment, a variable that is not well constrained by the exposed part of the fold. Trying a range of different detachment depths resulted in a wide range of necessary amounts of shortening and accompanying bed geometries (Figure 25). When constructing these folds, I restricted thickening to the hinge marked 'C' (Figure 25). Thickening in the other anticline hinge ('B') would result in a fanning of the beds in the backlimb, an effect not seen in the natural fold (but, interestingly enough, required by a rotating-limb fault-propagation fold as shown in the next section).

Of the resulting geometries, two were chosen as being reasonable starting points for further experimentation and form the basis for two variations of model A. The detachment fold with a depth to detachment of 3.5 units (Figure 25) shows a geometry with a small amount of thickening in the forward anticlinal hinge and an upward steepening of the forelimb, two features that are observed in the natural fold. This construction became the original detachment fold for model A, variation 1 (Figure 26). Using a depth to detachment of 5 units (Figure 25) generated a fold that is very near to a perfect parallel fold. This construction became the original detachment fold for model A, variation 2 (Figure 27). In this case, most steepening and thickness changes would have to be due to later fault-propagation folding.

In both variations of model A, the location and orientation of the hinges are largely unconstrained, given my base assumption of non-parallel folding. The hinges have been located somewhat arbitrarily to achieve a particular geometry.

Model A, variation 1: The fold grows from initially horizontal beds (Figure 26, stage 1) with fixed hinges and rotating limbs into a well-developed detachment fold (Figure 26, stage 2). At this point in the fold's evolution, a ramp cuts up section from a hypothesized lower flat. The ramp angle was set at 15 degrees as determined by field observations of the upper part of the ramp and placed such that it intersected the lowest marker bed at the forward synclinal hinge D (Figure 26). This was done to match the observed lack of a footwall syncline in any of the visible marker beds. A syncline would appear below the ramp in the beds beneath those shown, but if this variation is assumed to be correct, then the footwall syncline is buried and not visible in the natural fold.

Continued shortening leads to the geometry seen in stage 3 (Figure 26), at which point fault-propagation folding begins to be superimposed on the existing detachment fold geometry. This results in two significant features: 1) a noticeable kink forms in the backlimb over a bend between the hangingwall ramp and flat (Figure 26, 'a'); and 2) a new fold (Figure 26, 'b') forms at the base of the forelimb as a result of propagation of the ramp upward from a point near the lowest marker bed. The increased shortening also leads to a slight amount of thickening in the anticlinal crest and some steepening of the forelimb. The amount of shortening is not well constrained, but was chosen such that the resulting structure approximated that of the natural fold.

Model A, variation 2: As with variation 1, the fold forms from horizontal beds (Figure 27, stage 1) into a well-developed detachment fold with rotating limbs and fixed hinges (Figure 27, stage 2). The depth to detachment differs from variation 1 to better accommodate the ramp that forms in stage 3, so the geometry of the unaltered detachment fold also differs from that in variation 1. In stage 3 (Figure 27), a ramp begins to cut up section. The ramp was set to propagate from the point where the hindward backlimb hinge of the detachment fold ('A', Figure 27) meets the basal detachment, under the assumption that this would be a significant point of weakness. The ramp angle (34 degrees) was set so that the ramp intersects the bottom-most marker bed at hinge 'D' (Figure 27) and parallels bedding in the backlimb. This avoided a footwall syncline in any of the exposed marker beds, but again, a footwall syncline would be present in the subsurface. Up to this point, the fold has grown similarly to variation 1, with the differences in stage 3 of variations 1 and 2 resulting only from the initial difference in

depth to detachment. With an observed ramp angle of 15 degrees in the natural fold, however, an upward change in the ramp angle is required to successfully model the Yakataga anticline. This is done in stage 4 (Figure 27), at which point the ramp changes to a 15-degree dip. This spawns a new hinge above the point of the ramp angle change ('E', Figure 27) that tilts the anticlinal crest forward and steepens the forelimb. Non-parallel folding accommodates this 19-degree rotation in which the marker beds in the forelimb have simply been tilted forward as passive markers. The secondary fold seen in stages 3 and 4 (Figure 27) is caused by propagation of the ramp from a point near the lowest marker bed.

2) Model B: Rotating-limb fault-propagation fold

The Suppe and Medwedeff (1990) constant-thickness fault-propagation fold model is based on the assumption that the inclined layers have undergone only layer-parallel slip. In the Yakataga Formation, with few surfaces or competency contrasts along which slip could occur, it is unreasonable to expect that strain was accommodated in this manner. Previous research (Jamison, 1987; Mitra, 1990; Mosar and Suppe, 1992) has demonstrated the possibility of a layer-parallel strain gradient being accommodated in fault-propagation folds through thickening or thinning of the forelimb, resulting in limb rotation. However, in these instances thickness changes and rotation are all restricted solely to the forelimb. None of the fault-propagation fold models describe a kinematic history that includes a rotating backlimb, and for this reason they are not sufficient to model the Yakataga anticline.

However, if the effects of a shear gradient are not solely restricted to the forelimb and thickness changes are allowed to occur in the backlimb as well, a fault-propagation fold with a rotating backlimb can be envisioned. In essence, this can be thought of as an Epard and Groshong (1995) detachment fold forming above a ramp instead of a fixed, bed-parallel detachment horizon. In the previous models of fault-propagation folds with thickness changes in the forelimb (Jamison, 1987; Mitra, 1990; Mosar and Suppe, 1992), no rationale was given for restricting these changes to the forelimb, and I have to assume this was done simply because the models were easier to work with and quantify. It may also be that having the backlimb dip fixed by the ramp was an intuitive assumption that was never explicitly discussed, but in any case it certainly does not rule out the possibility of bed-length and bed-thickness changes being distributed across both limbs of the fold.

As with other fault-propagation fold models that allow thickness changes in the forelimb, I decided to use a shear gradient as my strain mechanism. Large amounts of shear strain are required, however, to get even a small amount of noticeable limb rotation when thickness changes are distributed across both limbs (Figure 28). If an initial ramp dip of 25 degrees is assumed, then the backlimb beds of the model need to rotate 10 degrees in order to match the dip of the beds in the natural fold. This initial ramp dip was chosen because it provides for the minimum amount of bed rotation required by the differences in dips across channel unconformities in the backlimb of the natural fold. I made the assumption that thickness changes (and the shear gradient) were restricted to the core of the fold, defined here as those beds that have been cut by the ramp. By working with an earlier, simpler version of the model that did not have a ramp angle

change (needed to match the observed geometry of the natural fold), I found that 60 degrees of shear were needed to get the necessary 10 degrees of backlimb rotation (Figure 28).

The model begins with undeformed, horizontal beds (Figure 29, stage 1). A lower detachment forms and starts cutting up section at a 25 degree dip. This results in a fault-propagation fold formed in accordance with the Suppe and Medwedeff model (1990), but modified to accommodate a shear gradient in both limbs (Figure 29, stage 2). As shear increases, it is taken up by thickening along the anticline hinge, resulting in rotation of both limbs. I have assumed that the shear is progressively added throughout fold development. Since stage 2 shows the fold at a late, but still incomplete, stage, I have only applied 50 degrees of shear at this point. As the ramp propagates upward from this point, it changes to a 15-degree dip in order to match the field observations. As shortening, fault propagation, and 10 more degrees of shear continue, the upper part of the fold forms into its current geometry (Figure 29, stage 3a), with the highest beds in the backlimb reaching a dip of 35 degrees. There is no aspect of the model that requires the formation of a secondary fold in the forelimb, as seen in both variations of model A. Since this feature is seen in the natural fold, I've included another step in the model (Figure 29, stage 3b) to allow a secondary fold to form. I hypothesize that this feature forms by gravitational collapse of material into the secondary fold due to over-steepening of the forelimb.

In summary, my final model for a rotating-limb fault-propagation fold (Figure 29) includes a ramp angle change and 60 degrees of shear resulting in forelimb and backlimb

rotation due to thickening. In the final stage (Figure 29, stage 3), the backlimb of the fold fans from an initial dip of 25 degrees above the ramp to 35 degrees in the highest beds of the fold core and above.

Comparison of the Models

Geometric-kinematic models cannot fully and accurately describe every aspect of a structure, and my intent with this project was not to offer a single definitive answer for the formation of the Yakataga anticline. The two pathways presented (models A and B) reasonably account for the major observations and interpretations of the natural fold, but do not rule out other possibilities. Certain areas pose problems with both the models and the natural fold. One of these is the region around the synclinal hinge. In the natural fold, beds dip steeply and are affected by the secondary fold in the lower part of the forelimb, but higher up section are not faulted or affected by the secondary fold and are simply curved into the syncline (Figure 7). This creates some space problems in the syncline hinge. Some of this could possibly be accounted for by back-thrusting and duplexing of the beds directly above the fault tip, causing some of the thickening seen in the syncline hinge in the final stage of model B (Figure 29). The presence of a prominent back-thrust above the ramp tip (Figure 8) and the observations of backthrusts above triangle zones in other areas lend some credence to this idea. It is more likely, however, that the geometry of the uppermost unconformity solves this space problem (Figure 30). Photographs of the forelimb region (Figure 10, 12, and 13) suggest that the uppermost unconformity can be traced from the fold crest across the hinge to the angular unconformity documented in

the forelimb and then down to the area of truncated beds above the ramp tip. If this is true, then the unconformity simply truncates the secondary fold and allows the stratigraphically higher beds to remain unaffected by the secondary fold (Figure 30).

This interpretation has implications for the models. Given the concordance of overlying beds to the unconformity surface in the fold's forelimb (Figure 12), the unconformity must have formed prior to a significant amount of forelimb steepening. With an angular difference of 42 degrees between the beds stratigraphically above and below the unconformity, the forelimb could not yet have been overturned at the time that the unconformity formed. However, if the unconformity does truncate the secondary fold in the forelimb, then it must have formed after the secondary fold formed. Model B (Figure 29) has no requirement for the formation of this feature, but I speculated that it would have formed in this instance due to oversteepening of the forelimb and accompanying gravitational collapse, a necessarily late event that is inconsistent with this interpretation. Model A (Figures 26 and 27) is also inconsistent, as the secondary fold is only shown to have formed after the forelimb had steepened considerably. However, these models could be altered to accommodate earlier formation of the secondary fold in the forelimb, a step that is beyond the scope of the present project and will have to remain for future work.

It is difficult to account for a rotating backlimb above a fault ramp while still adhering to a kinematic scheme based on the Suppe and Medwedeff (1990) fault-propagation fold or other models that account for changes in the forelimb but not the backlimb (e.g., Mitra, 1990). Having the backlimb dip fixed by the ramp dip is not only a

simple way to construct cross sections, but it is also an intuitive result of pushing originally horizontal beds up a ramp. This relationship has certainly been recognized as long ago as the oft-cited study of the Pine Mountain thrust sheet by J.L. Rich in 1934, and existed as an informal concept long before the formal introduction of the terms "fault-bend fold" (Suppe, 1983) and "fault-propagation fold" (Mitra, 1990; Suppe and Medwedeff, 1990). Strain accommodation through backlimb thickening is the only mechanism I was able to conceive of to allow for backlimb rotation above a ramp. Assuming this happens due to a shear gradient as in model B (Figure 29), then the amounts of shear needed to obtain the necessary rotation seem implausible. If the Yakataga Formation had undergone 60 degrees of shear, I would have expected to see some evidence of this in the field. In addition, the fanning of beds required by the model is absent in the Yakataga anticline, where the backlimb dips are constant except where they change abruptly across unconformity surfaces.

Superimposing a cross-section of the Yakataga anticline over the final stage of model B (Figure 31) serves to assess the overall agreement, or lack thereof, between the model and the natural fold. A big discrepancy in the location of the ramp relative to the fold core exists between the two and the forelimb in the model is too steep. This lack of agreement, coupled with the implausibility of 60 degrees of shear without obvious effects in the limbs, leads me to reject model B.

Other researchers who have abandoned the simple kink-geometry of common fault-propagation fold models have had success representing natural fold geometries with the Erslev (1991) trishear model (Erslev and Mayborn, 1997; Ford and others, 1997).

The trishear model "incorporates distributed deformation in a triangular shear zone [attached to a fault tip] and non-rigid limb rotation" (Ford and others, 1997, p.) (Figure 32). The trishear model might help address some of the complications in the forelimb, but as with other fault-propagation fold models, it does nothing to account for rotation of the backlimb.

Of the two models presented, then, I prefer model A, the detachment fold overprinted by fault-propagation folding. Superimposing the cross-section of the natural fold over the final stages of variations 1 and 2 (Figures 31) shows much better agreement in both cases than seen with model B. However, the location of the ramp relative to the fold core is off in the models (less so in variation 1, and in both cases less than in model B). In variation 1, the backlimb kink developed in the model should have been visible in outcrop, based on its position relative to the cross section of the natural fold. In variation 2, the hindward syncline hinge is located where these beds should have been visibly folded in the backlimb. Neither variation 1 or 2 agrees completely in the forelimb. The forelimb of the natural fold is interpreted to be fanning, with the stratigraphically higher beds steeply overturned. In variation 1, the forelimb dips agree well with the beds closest to the fold core, and in variation 2 the forelimb dips agree well with beds higher in the succession. Despite these differences, there is a good general agreement in both cases.

The general concept of a thrust cutting a pre-existing fold is nothing new, dating back at least as far as the Willis (1893) break-thrust fold. Invoking a rotating-limb detachment fold model like that of Epard and Groshong (1995) accounts for the rotation required by the backlimb channel deposits, and the later fault-propagation serves to create

a secondary fold in the forelimb and accounts for some of the non-parallel steepening seen in the forelimb. Neither of the two variations provides perfect matches, but I prefer variation 2 based on the location of the base of the ramp. In this case, the origin of the ramp at a natural point of weakness (fold hinge) makes intuitive sense. A better fit to the natural fold could probably be attained through further refinements to the model. This might incorporate the best aspects of each variation, such as the limb thickening of variation 1 and the change in ramp dip of variation 2. The ramp could be moved downward for a better fit, and detachment depth could be increased for a better match in the backlimb.

Kinematic vs. Mechanical Models

Geometric/kinematic modeling of folds has been a common technique for some time now and this was the approach I took to explain how the Yakataga anticline formed. Kinematic modeling generally produces a series of pictures that represent time slices of the motions involved. These slices are generally constrained by geometric observations of the structure, and the principles of area and/or line balancing. If the models balance, restore to a geologically reasonable state, and match the observed geometry, they are deemed to be allowable (although often this is mistaken to mean "correct"). This methodology was recently called into question in a paper by Fletcher and Pollard (1999), which doubted the validity of any model that did not rely on "causative physical principles." Their mechanical approach to structural processes consists of forward modeling based on explicit boundary and initial conditions along with the fundamental

laws of physics. This approach has its own limitations, however, particularly related to how one constrains the initial and boundary conditions and determines quantitative descriptions of materials behavior under true geologic conditions and over true geologic time. But Fletcher and Pollard do raise some important issues: "An attempted link is often made… between results for an ad hoc kinematic model, in which physics plays no part, and intuitive ideas as to process. However plausible these may seem, they provide no substantive basis for further investigation because the relevant physical quantities (stress, constitutive properties, friction) are absent in the ad hoc model" (Fletcher and Pollard, 1999).

I agree that a complete description and model of a fold must take into account the mechanics, but I also think that using a complete mechanical model as the first step is risking unrealistically overly simplifying the situation as well, not to mention that you must have a rigorous description of what you are trying to match with a model in the first place. I see the mechanical approach as an important future step (or a simultaneous collaboration with a mechanist if the opportunity is available), but still see the importance of incorporating into mechanical modeling the geometric constraints and information, no matter how intuitive or qualitative, that can be reconstructed from natural folds and derived from kinematic models.

Conclusions

None of the current thrust-related fold models fully account for all of the observed features of the Yakataga anticline. The presence of a ramp tip and a gross fold geometry

that includes a steeply dipping to overturned forelimb suggests applicability of one of the fault-propagation fold models. However, the discordance across channel unconformities suggests that the backlimb has rotated during fold growth, which contradicts any of the existing fault-propagation fold models. The current detachment fold models can also account for the fold geometry and allow for rotating limbs, but none accommodates a ramp tip. I offer two general models for the Yakataga anticline: 1) model A, a detachment fold that was cut late in its development by a ramp and deformed by fault-propagation folding (Figures 26 and 27); and 2) model B, a rotating-limb fault-propagation fold, with rotation occurring due to limb and hinge thickening caused by a shear gradient (Figure 29). Of these two models, I prefer the detachment fold modified by later fault-propagation folding, since the rotating-limb fault-propagation fold results in a fanning of backlimb dips that was not observed in the natural fold and requires an implausibly high amount of layer-parallel shear. This is not to say that my preferred model is the only correct solution to the problem, but it does exist as a possible kinematic pathway different from the current thrust-related models. This serves to illustrate the importance of testing models before blindly applying them to areas where they may not be relevant. Too often models are used as "black boxes" that spit out answers accepted as correct, without adequate examination of the applicability of the models to the natural structures of the area in question. In areas of young, weakly consolidated and mechanically homogeneous sediments, the familiar fault-propagation fold models may not be applicable even when many aspects of the geometry are consistent with them.

References

Armentrout, J.M., 1983, Glacial lithofacies of the Neogene Yakataga Formation, Robinson Mountains, southern Alaska Coast Range, Alaska, *in* Molina, B.F., ed., Glacial-marine sedimentation: Plenum Press, New York, p. 629-666.

Bruns, T.R., 1983, Model for the origin of the Yakutat block, an accreting terrane in the northern Gulf of Alaska: Geology, v. 11, p. 718-721.

Bruns, T.R., 1985, Tectonics of the Yakutat block, an allochthonous terrane in the northern Gulf of Alaska: United States Department of the Interiror, Geological Survey, Open-file report 85-13.

Chester, J.S., and Chester, F.M., 1990, Fault-propagation folds above thrusts with constant dip: Journal of Structural Geology, v. 12, p. 903-910.

Davis, D.M., and Lillie, R.J., 1994, Changing mechanical response during continental collision: active examples from the foreland thrust belts of Pakistan: Journal of Stuctural Geology, v. 16, p. 21-34.

De Paor, D.G., 1988, Balanced section in thrust belts; Part 1: Construction: The American Association of Petroleum Geologists Bulletin, v. 72, no. 1, p. 73-90.

Epard, J.L., and Groshong Jr., R.H., 1995, Kinematic model of detachment folding including limb rotation, fixed hinges and layer-parallel strain: Tectonophysics, v. 247, p. 85-103.

Erslev, E.A., 1991, Trishear fault-propagation folding: Geology, v. 19, p. 617-620.

Erslev, E.A., and Mayborn, K.R., 1997, Multiple geometries and modes of fault-propagation folding in the Canadian thrust belt: Journal of Structural Geology, v. 19, Nos. 3-4, p. 321-335.

Eyles, C.H., Eyles, N., Lagoe, M.B., 1991, The Yakataga Formation; A late Miocene to Pleistocene record of temperate glacial marine sedimentation in the Gulf of Alaska, *in,* Anderson, J.B., and Ashley, G.M., eds., Glacial marine sedimentation; Paleoclimatic significance: Geological Society of America Special Paper 261, p. 159-180.

Eyles, C.H., and Lagoe, M.B., 1998, Slump-generated megachannels in the Pliocene-Pleistocene glaciomarine Yakataga formation, Gulf of Alaska: Geological Society of America Bulletin, v. 110, no. 3, p. 395-408.

Fischer, M.P., and Jackson, P.B., 1999, Stratigraphic controls on deformation patterns in fault-related folds: a detachment fold example from the Sierra Madre Oriental, northeast Mexico: Journal of Structural Geology, v. 21, p. 613-633.

Fischer, M.P., Woodward, N.B., and Mitchell, M.M., 1992, The kinematics of break-thrust folds: Journal of Stuctural Geology, v. 14, No. 4, p. 451-460.

Fletcher, R.C., and Pollard, D.D., 1999, Can we understand structural and tectonic processes and their products without appeal to a complete mechanics?: Journal of Structural Geology, v. 21, p. 1071-1088.

Ford, M., Williams, E.A., Artoni, A., Verges, J., and Hardy, S., 1997, Progressive evolution of a fault-related fold pair from growth strata geometries, Sant Llorenc de Morunys, SE Pyrenees: Journal of Structural Geology, v. 19, p. 413-441.

Homza, T.X., and Wallace, W.K., 1995, Geometric and kinematic models for detachment folds with fixed and variable detachment depths: Journal of Structural Geology, v. 17, p. 575-588.

Homza, T.X., and Wallace, W.K., 1997, Detachment folds with fixed hinges and variable detachment depth, northeastern Brooks Range, Alaska: Journal of Structural Geology, v. 19, nos. 3-4, p. 337-354.

Hyett, A.J., 1990, Deformation around a thrust tip in Carboniferous limestone at Tutt Head, near Swansea, South Wales: Journal of Structural Geology, v. 12, p. 47-58.

Jamison, W.R., 1987, Geometric analysis of fold development in overthrust terranes: Journal of Structural Geology, v. 9, no. 2, p. 207-219.

Mitra, S., 1990, Fault-propagation folds: geometry, kinematic evolution, and hydrocarbon traps: The American Association of Petroleum Geologists Bulletin, v. 74, no. 6, p. 921-945.

Mosar, J., and Suppe, J., 1992, Role of shear in fault-propagation folding, *in* McClay, K.R., ed., Thrust Tectonics: Chapman and Hall, London, p. 123-132.

Passchier, C.W., Trouw, R.A., Zwart, H.J., and Vissers, R.L.M., 1992, Porphyroblast rotation: eppur si muove?: Journal of Metamorphic Geology, v. 12, p .403-417.

Pfiffner, O.A., 1993, The structure of the Helvetic nappes and its relation to the mechanical stratigraphy: Journal of Structural Geology, v. 15, p. 511-521.

Plafker, G., 1987, Regional geology and petroleum of the northern Gulf of Alaska continental margin, in Scholl, D.W., Grantz, A., and Vedder, J.G., eds., Geology and resource potential of the continental margin of western North America and adjacent ocean basins: Circum-pacific Council for Energy and Mineral Resources, Earth Sciences series, v. 6, p. 229-268.

Poblet, J., and Hardy, S., 1995, Reverse modelling of detachment folds; application to the Pico del Aguila anticline in the South Central Pyrenees (Spain): Journal of Structural Geology, v. 17, no. 12, p. 1707-1724.

Poblet, J., and McClay, K., 1996, Geometry and kinematics of single-layer detachment folds: AAPG Bulletin, v. 80, p. 1085-1109.

Poblet, J., McClay, K., Storti, F., and Munoz, J.A., 1997, Geometries of syntectonic sediments associated with single -layer detachment folds: Journal of Structural Geology, v. 19, nos. 3-4, p. 369-381.

Poblet, J., Munoz, J.A., Trave, A., Serra-Kiel, J., 1998, Quantifying the kinematics of detachment folds using three-dimensional geometry: Application to the Mediano anticline (Pyrenees, Spain): Geological Society of America Bulletin, v. 110, p. 111-125.

Ramsay, J.G., and Huber, M.I., 1987, Fold mechanics: 2. Multilayers *in* The Techniques of Modern Structural Geology, Volume 2: Folds and Fractures, p. 405-444.

Rich, J.L., 1934, Mechanics of low angle overthrust faulting as illustrated by the Cumberland thrust block, Virginia, Kentucky, and Tennessee: Bulletin of the American Association of Petroleum Geologists, v. 18, p. 1584-1596.

Suppe, J., 1983, Geometry and kinematics of fault-bend folding: American Journal of Science, v. 293, p. 684-721.

Suppe, J., and Medwedeff, D.A., 1990, Geometry and kinematics of fault-propagation folding: Eclogae Geologicae Helvetiae, v. 83, p. 409-454.

Thorbjornsen, K.L., and Dunne, W.M., 1997, Origin of a thrust-related fold: geometric vs kinematic tests: Journal of Structural Geology, v. 19, Nos. 3-4, p. 303-319.

Willis, B., 1893, Mechanics of Appalachian Structure. US Geological Survey Annual Report 13 (1891-1892), part 2, p. 217-281.

Woodward, N.B., and Rutherford, E., Jr., 1989, Structural lithic units in external orogenic zones: Tectonophysics, v. 158, p. 247-267.

Zapata, T.R., and Allmendinger, R.W., 1996, Growth stratal records of instantaneous and progressive limb rotation in the Precordillera thrust belt and Bermejo basin, Argentina: Tectonics, v. 15, p. 1065-1083.

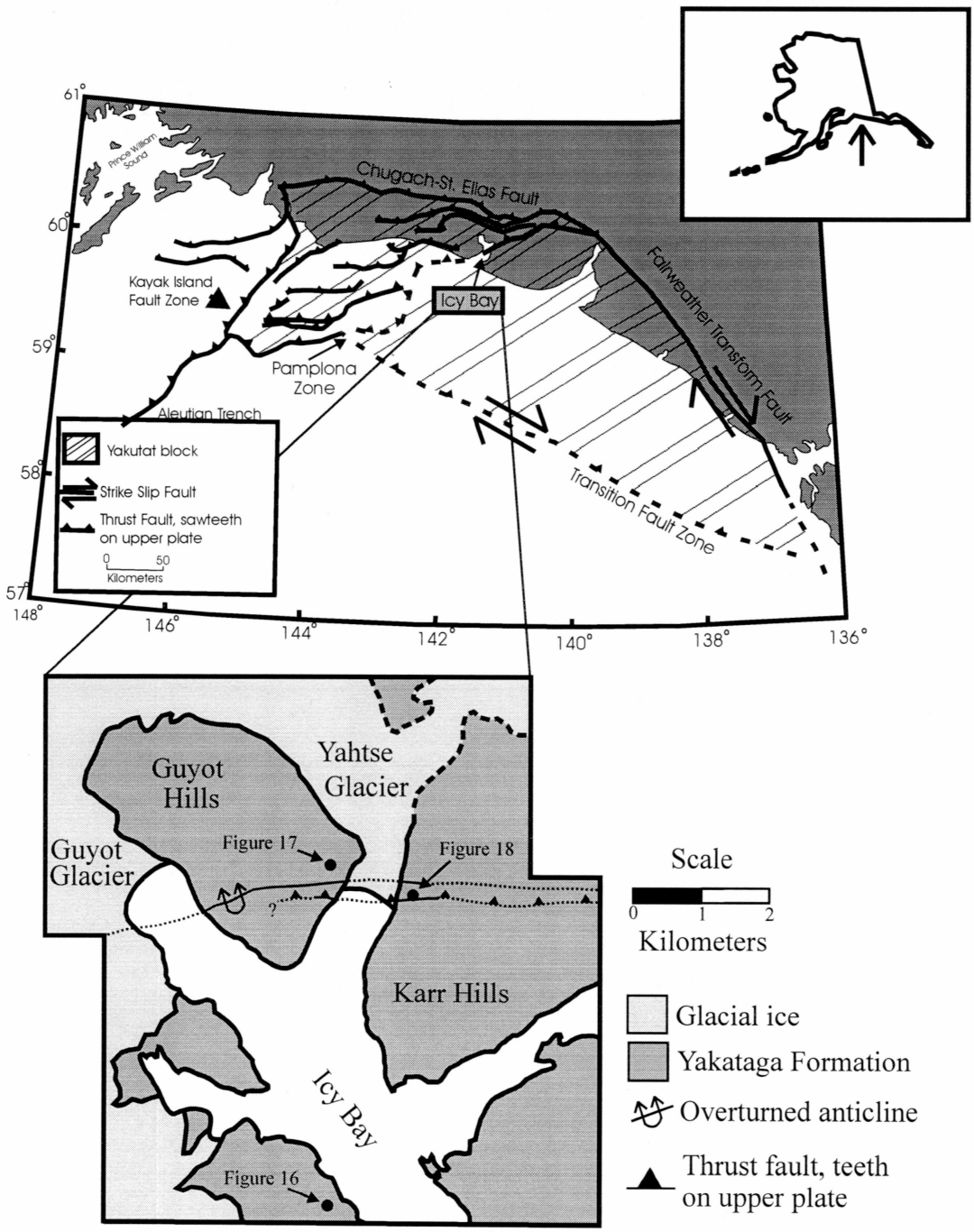

Figure 1, **Location Map**: Location map showing generalized structure of the northeastern Gulf of Alaska. Diagonal lines delineate the Yakutat block. The blow-up is of Icy Bay with the location of the fold hinge marked. Black dots show the location of stratigraphic columns presented later in the text. Modified from Bruns (1985) and Eyles and others (1991).

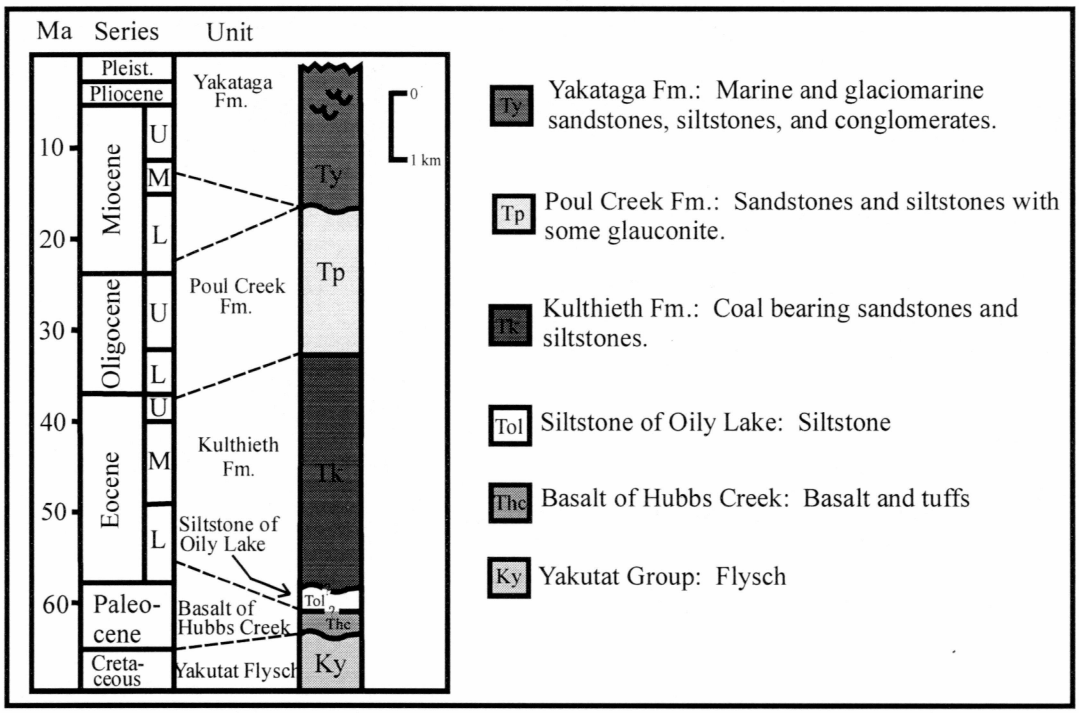

Figure 2, **Regional Stratigraphy**: Stratigraphic units from the central part of the Yakutat terrane, included to show the relationship of the Yakataga Formation to underlying units. Modified from Plafker, 1987.

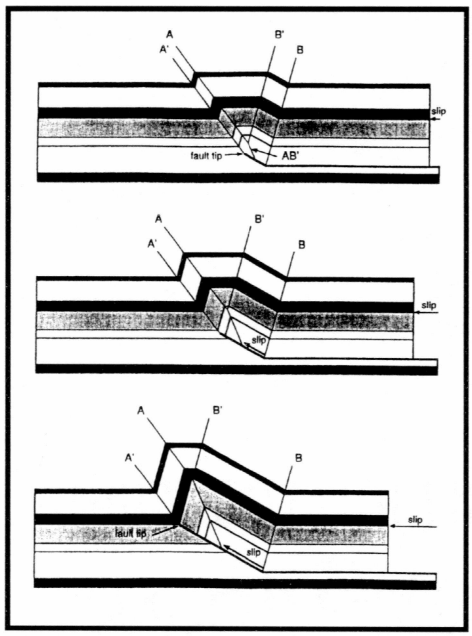

Figure 3, **Fault-propagation fold model**: The progressive development of a fault-propagation fold. The model predicts a back-limb dip that is fixed by the angle of the fault ramp. From Suppe and Medwedeff (1990).

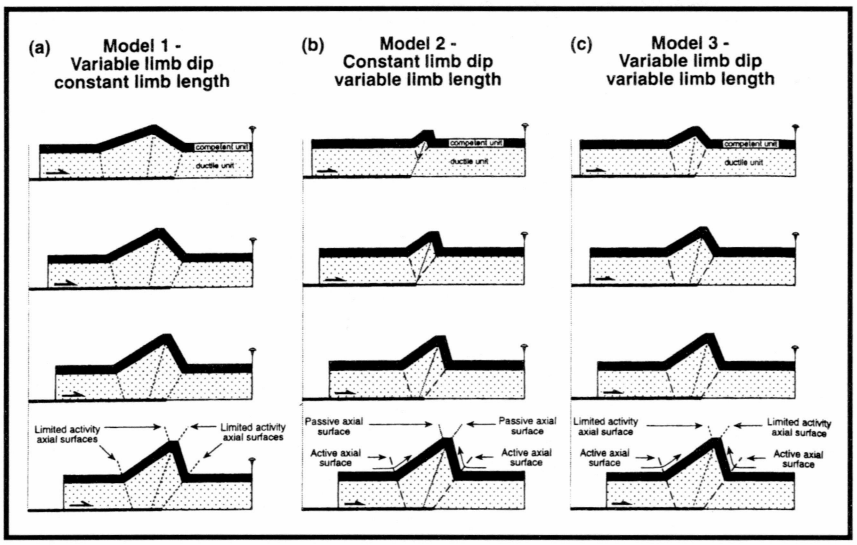

Figure 4, **Detachment fold model**: Three different kinematic models for detachment folds. Models (a) and (c) allow for rotation of both forelimbs and backlimbs. From Poblet and others, 1997.

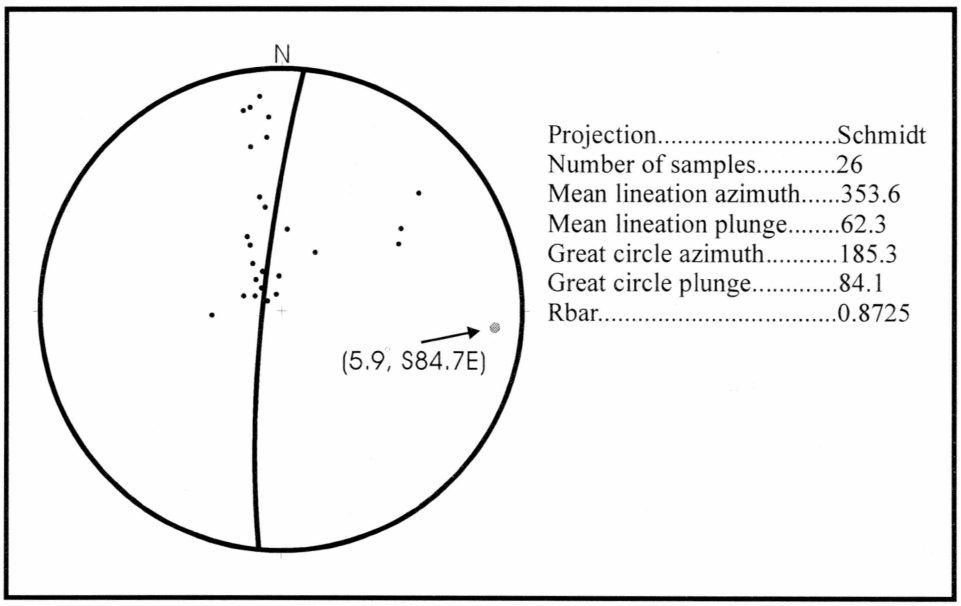

Figure 5, **Plotted bedding attitudes**: Bedding attitudes collected from around the syncline and plotted on a pi diagram. Shows the trend and plunge of the syncline hinge to be 5.9 degrees, 95.3 degrees azimuth. This is based on only 26 attitudes, but is in agreement with estimates made in the field (trending N80E with a plunge of

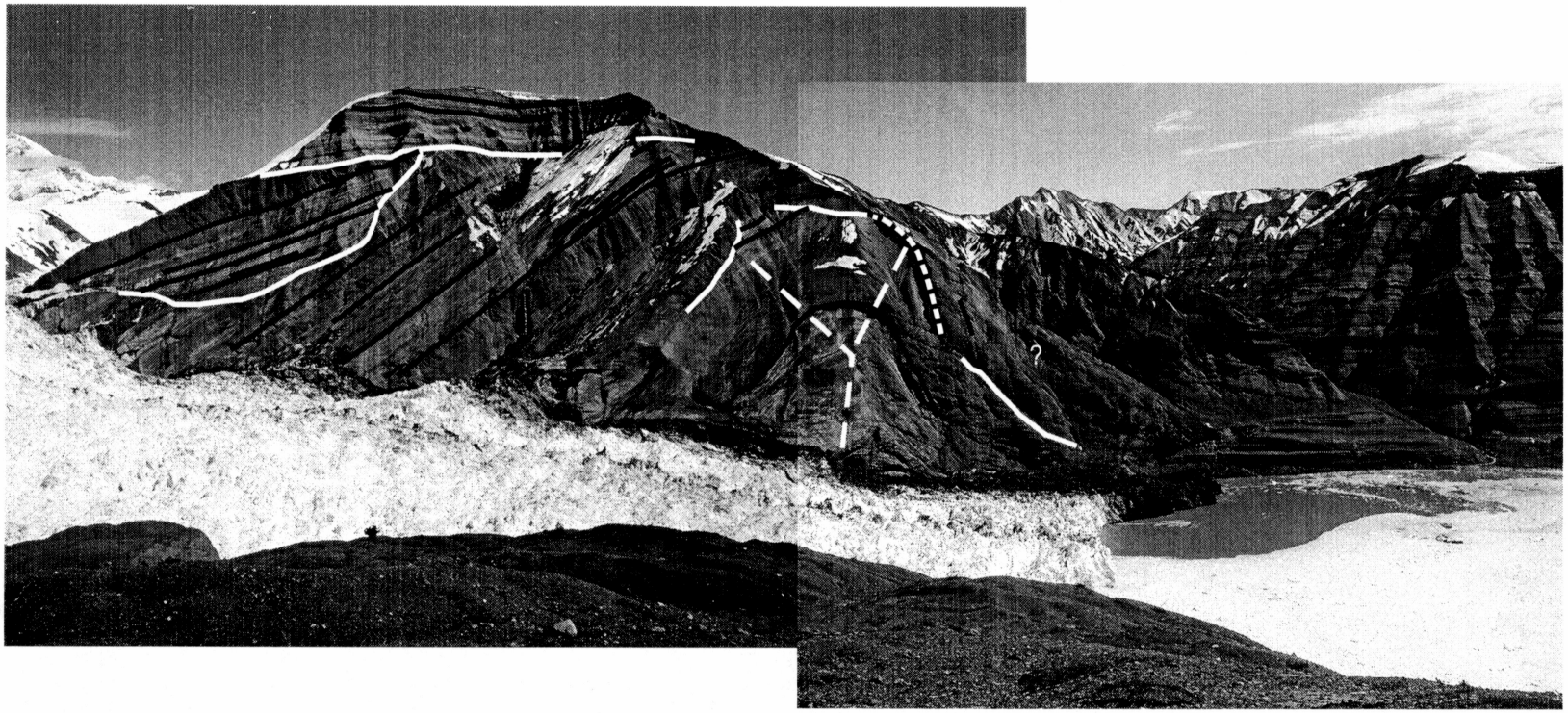

Figure 6a, **Yakataga anticline overview**: Composite panorama of the Yakataga anticline as seen in the Karr Hills, taken from the Guyot Hills looking east. Black lines trace out bedding, white lines show channel unconformities, and the white dashed lines shows the branching axial surface. Photo was taken looking east from the neighboring Guyot Hills, and is from a perspective nearly along strike with the backlimb of the fold. Highest elevations seen are at 4000 feet, and the scale of the photo from right to left is approximately 1.5 miles.

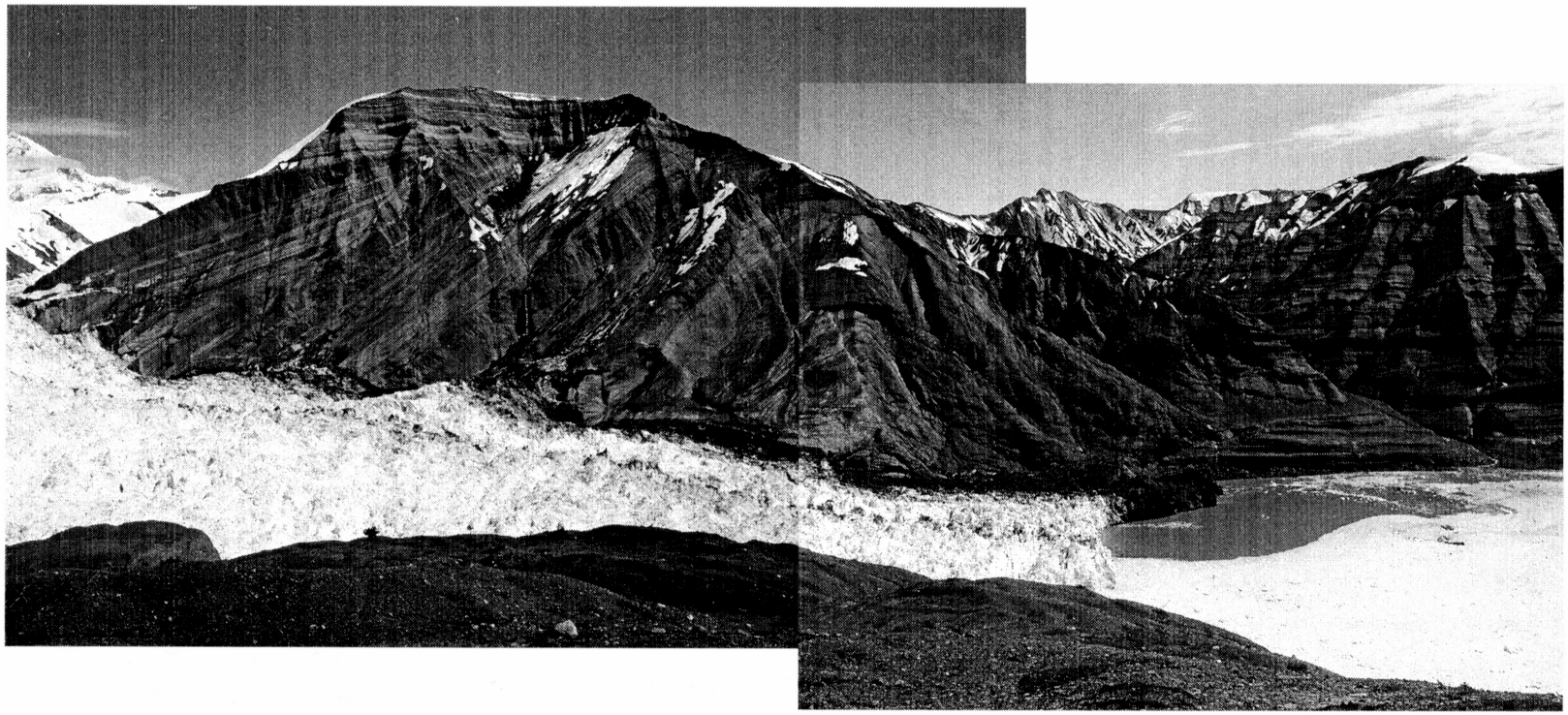

Figure 6b, **Yakataga anticline overview**: Uninterpreted photo of the Yakataga anticline.

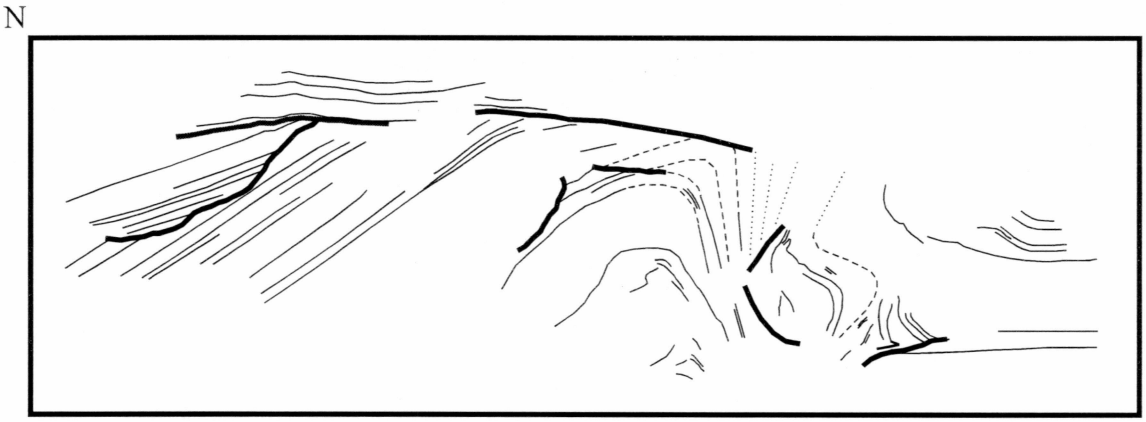

Figure 7, **Cross section of the Yakataga anticline**: Compiled from oblique photos and airphotos of the region. Heavy black lines represent channel unconformity surfaces, except in the case of the fault, which is marked by an arrow. Solid black lines represent bedding. Dashed and dotted lines also represent bedding, but with a decreasing degree of certainty.

Figure 8a, **Overview of ramp tip**: Interpreted photo of the area surrounding the fault tip. Faults are shown as heavy white lines and bedding is shown as thin white lines. Both are dashed where inferred.

Figure 8b, **Overview of ramp tip**: Uninterpreted photo of the area surrounding the fault tip.

Figure 9, **Close-up of ramp tip**: Photo showing fractures on either side of thrust near the tip (fault tip is just out of view to the right). Without any distinct marker beds, the exact nature of the fractures in both the hanging wall and the footwall is unclear. Scale of photo is approximately 1 meter from top to bottom.

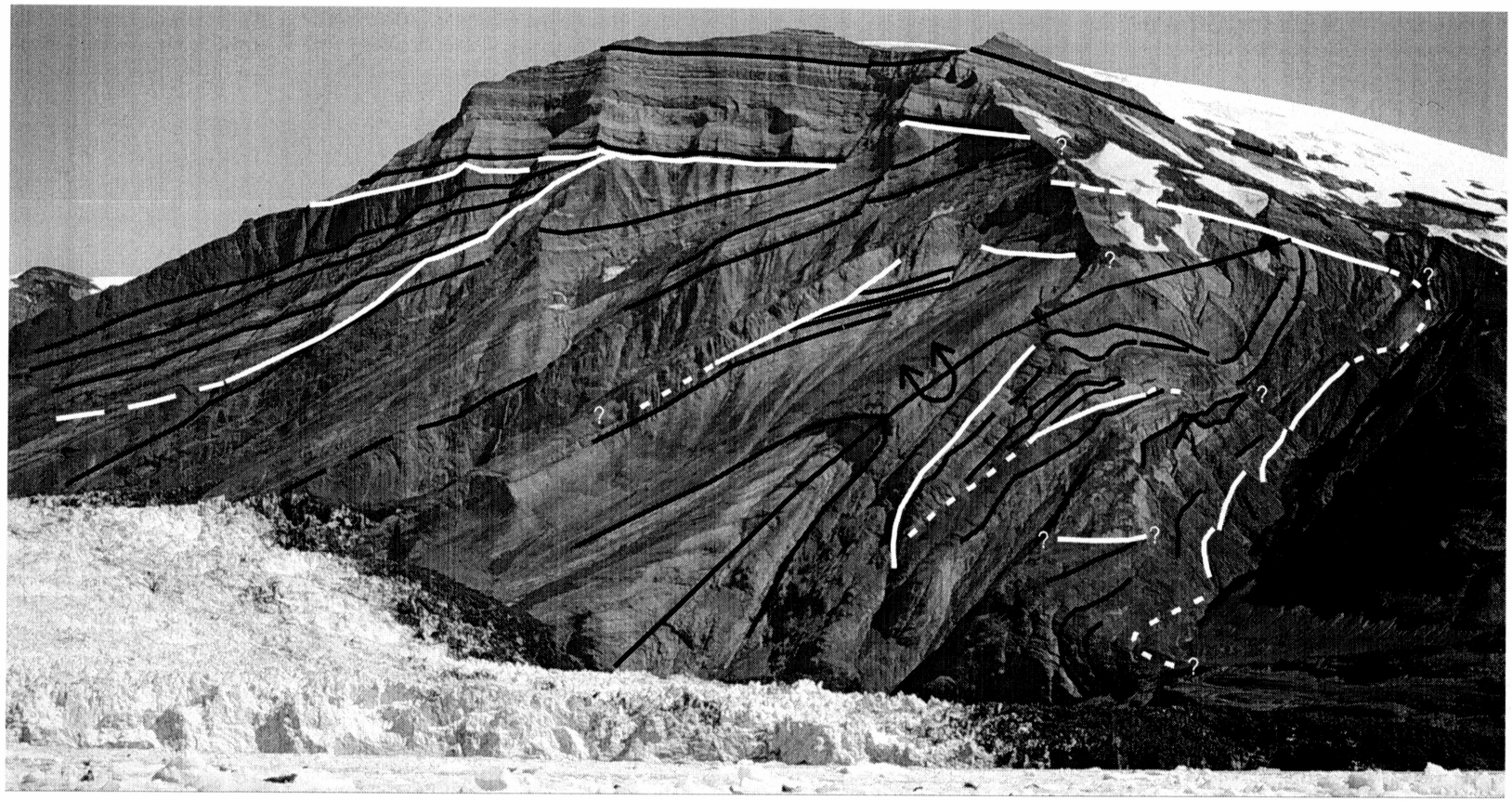

Figure 10a, **Yakataga anticline overview**: An oblique view of the fold, with more detail visible in the forelimb. Photo taken from the water in the Yahtse fjord, looking NE. Black lines trace out bedding, white lines trace out unconformities (interpreted to be channel surfaces), and the fold axial trace is marked by the over-turned anticline symbol.

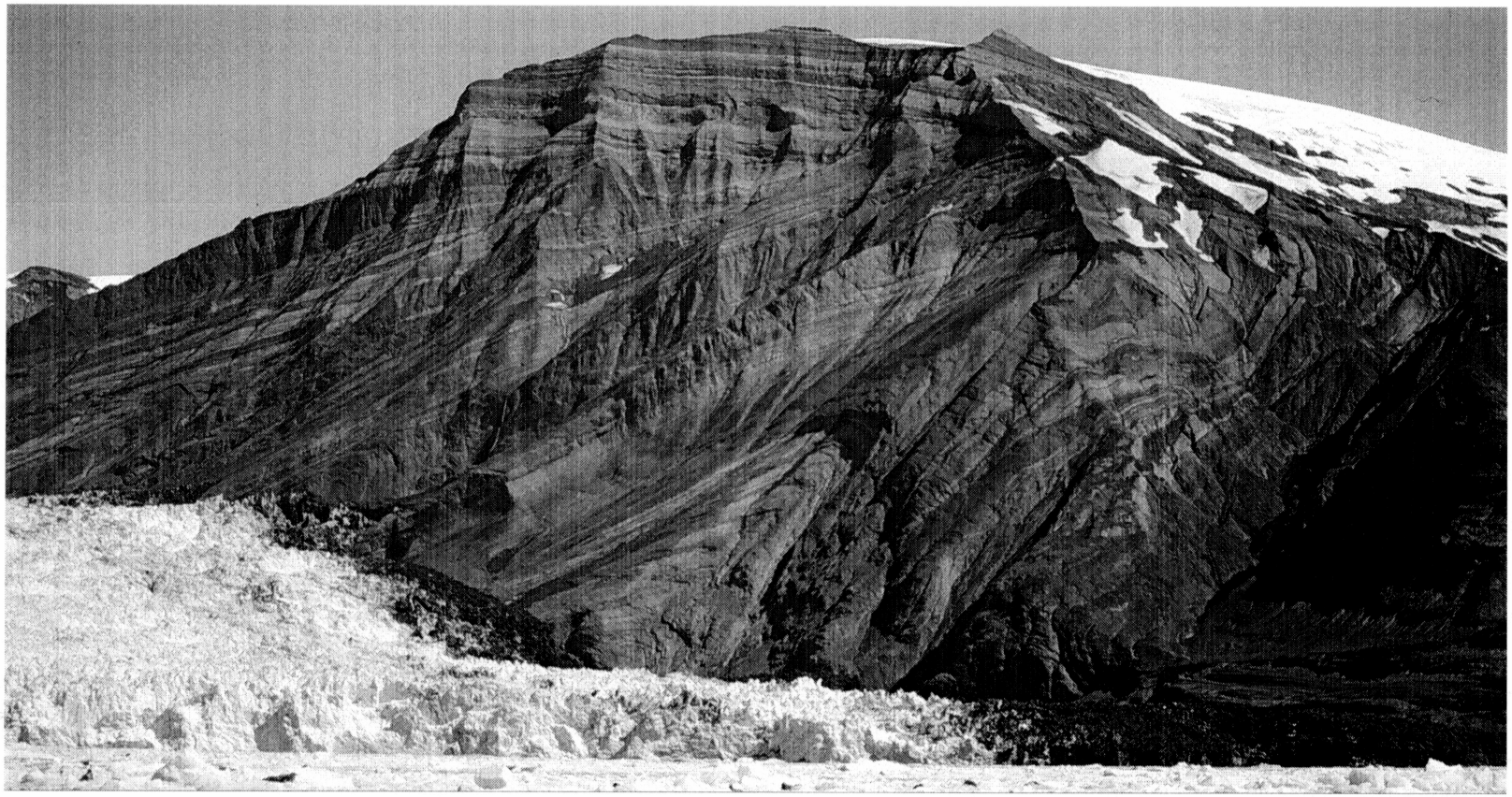

Figure 10b, **Yakataga anticline overview**: Uninterpreted photo of the Yakataga anticline.

Figure 11a, **Close-up of backlimb**: Close-up of the prominent backlimb unconformity visible in figure 6. Black lines trace out bedding, white lines show an unconformity surface. Taken from a vantage point nearly along strike, looking east.

Figure 11b, **Close-up of backlimb**: Uninterpreted photo of the backlimb.

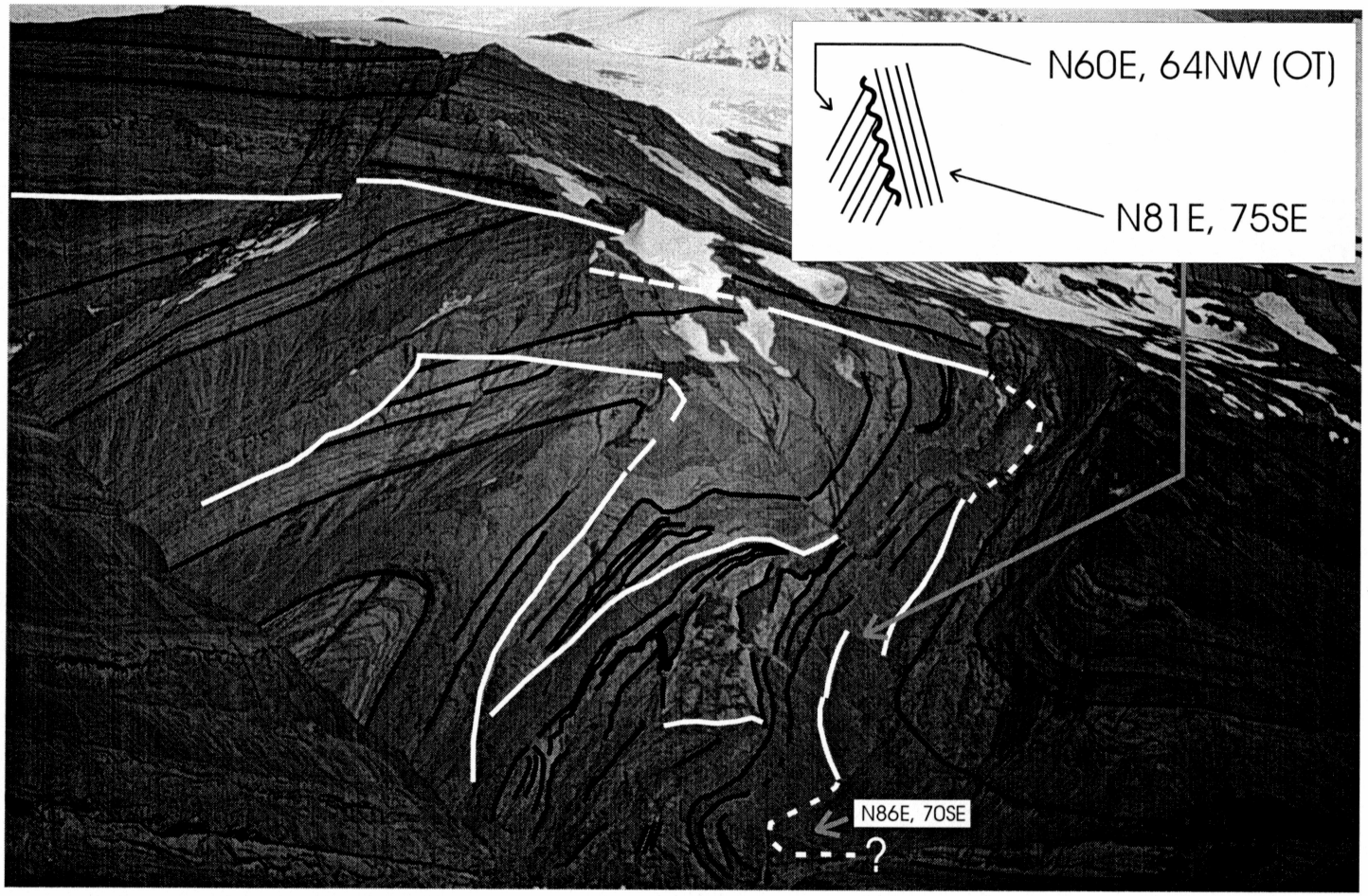

Figure 12a, **Overview of forelimb**: Telephoto view, showing the complicated depositional and deformational geometry of the bedding. Black lines trace out bedding, white lines show unconformities. Photo taken looking ENE towards the Karr Hills, with the toe of the Guyot Hills just visible in the left foreground. Inset showing the unconformity is based on field observations, and lower inset with the strike and dip measurement gives a typical attitude from this part of the fold.

Figure 12b, **Overview of forelimb**: Uninterpreted photo of the forelimb area.

Figure 13a, **Close-up of forelimb**: Higher-power telephoto view of the forelimb area shown in Figures 10 and 12. Black lines trace out bedding, white lines show unconformities. The bed marked "Bed A" is included to help illustrate the apparent offset due to the topography of a ridge with a hidden gully behind it. The ridge is highlighted by the black line of alternating dots and dashes.

Figure 13b, **Close-up of forelimb**: Uninterpreted photo of the forelimb area.

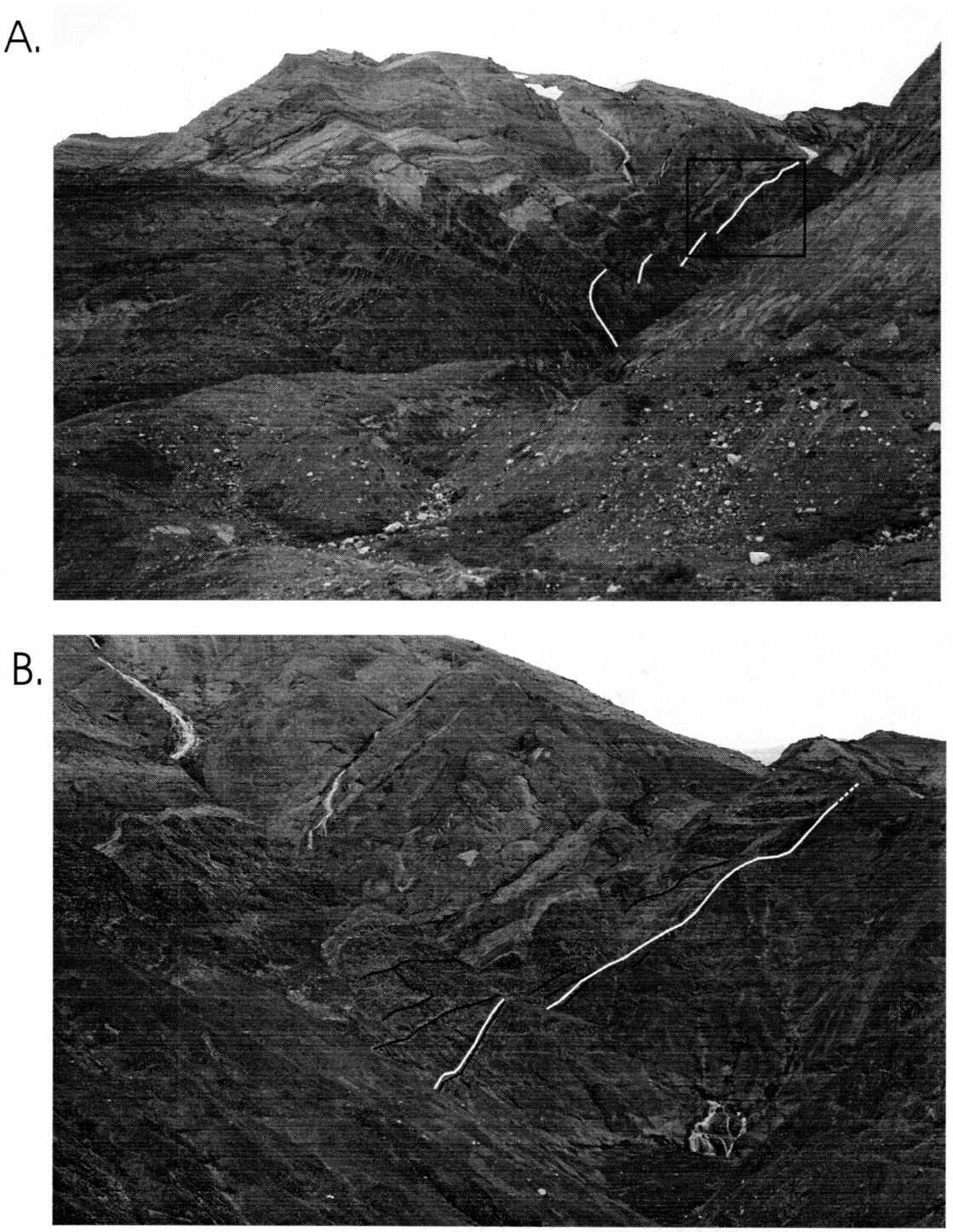

Figure 14, **Forelimb unconformity location**: Location of the prominent angular unconformity in the forelimb that can be traced to a point just below the fold hinge. B is a closeup of the area outlined by the black box in A. White line traces the unconformity, black lines trace out bedding.

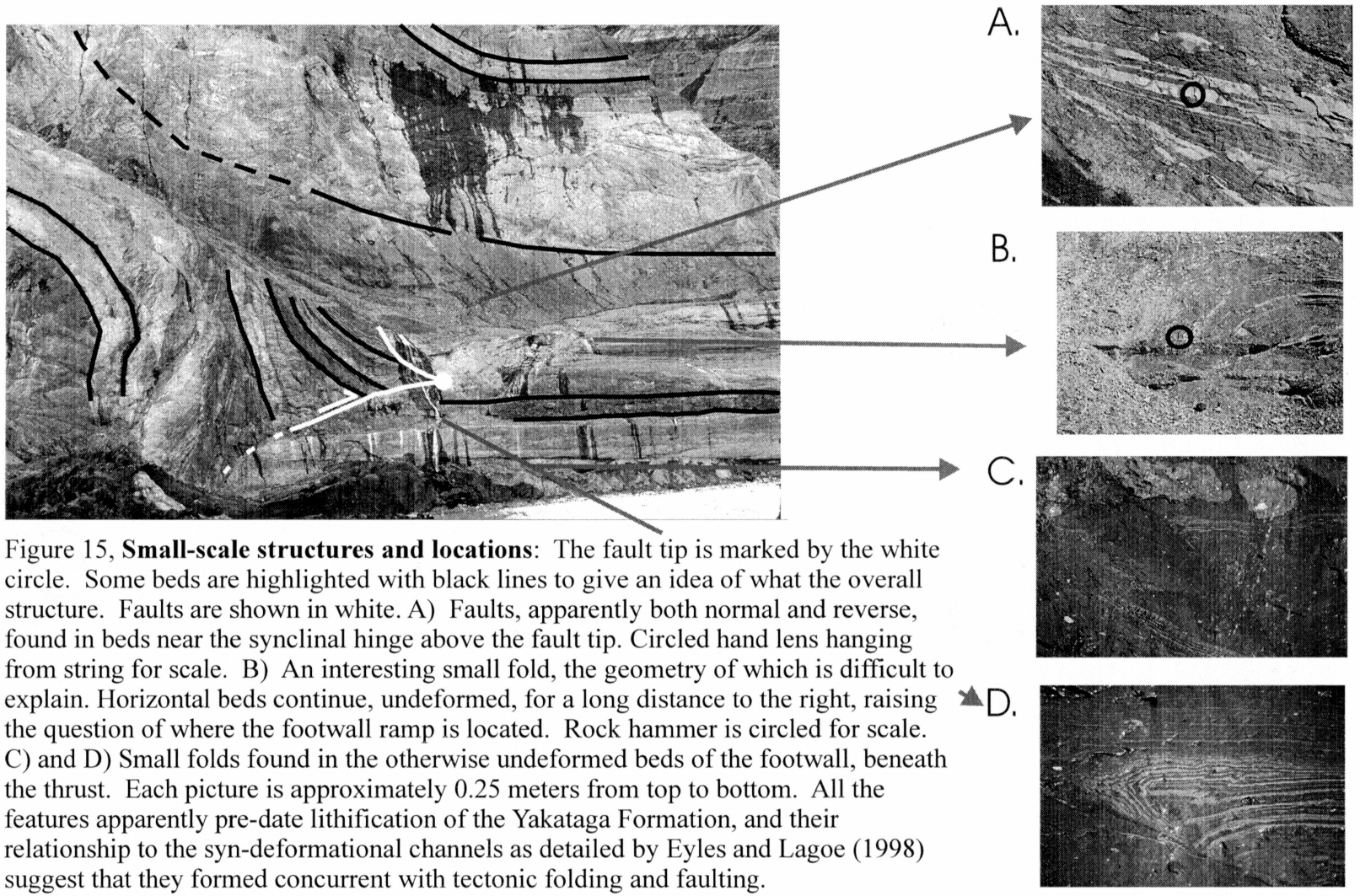

Figure 15, **Small-scale structures and locations**: The fault tip is marked by the white circle. Some beds are highlighted with black lines to give an idea of what the overall structure. Faults are shown in white. A) Faults, apparently both normal and reverse, found in beds near the synclinal hinge above the fault tip. Circled hand lens hanging from string for scale. B) An interesting small fold, the geometry of which is difficult to explain. Horizontal beds continue, undeformed, for a long distance to the right, raising the question of where the footwall ramp is located. Rock hammer is circled for scale. C) and D) Small folds found in the otherwise undeformed beds of the footwall, beneath the thrust. Each picture is approximately 0.25 meters from top to bottom. All the features apparently pre-date lithification of the Yakataga Formation, and their relationship to the syn-deformational channels as detailed by Eyles and Lagoe (1998) suggest that they formed concurrent with tectonic folding and faulting.

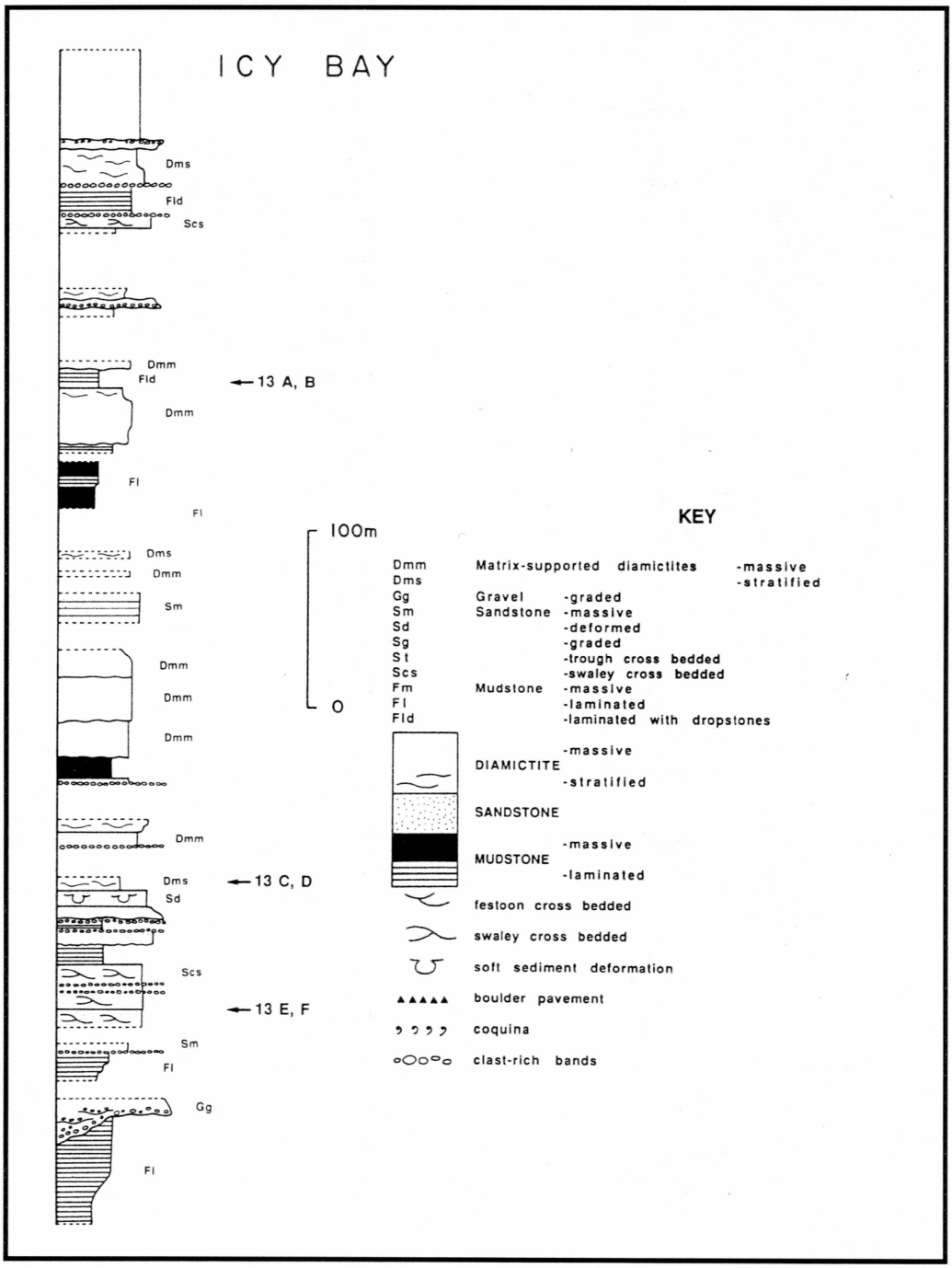

Figure 16, **Lower Icy Bay stratigraphy**: Sedimentological logs through the lower Yakataga Formation sediments of Icy Bay. Location of section marked on figure 1. From Eyles and others (1991).

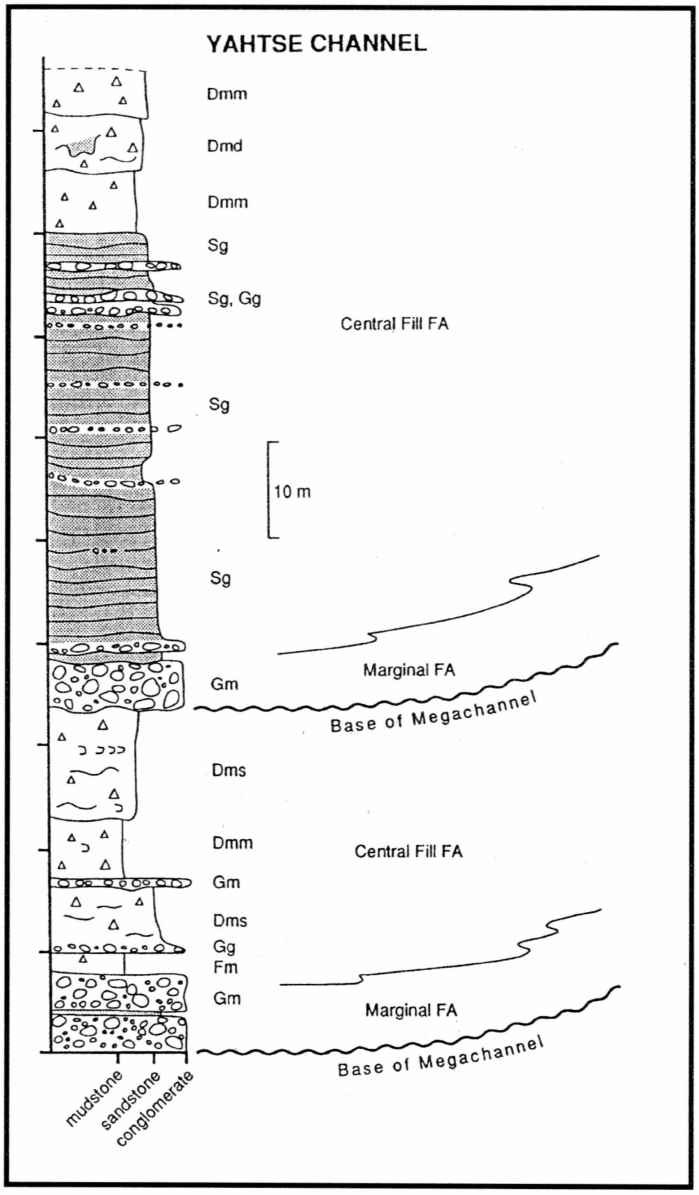

Figure 17, **Upper Icy Bay stratigraphy**: Measured section from Eyles and Lagoe (1998). Taken from the Guyot Hills (location marked in figure 1). Codes and symbols as from figure 16 with the addition of: Dmd = Diamictite, matrix supported, deformed; Gm = Conglomerate, massive. Section occurs higher in the Icy Bay succesion than Figure 16.

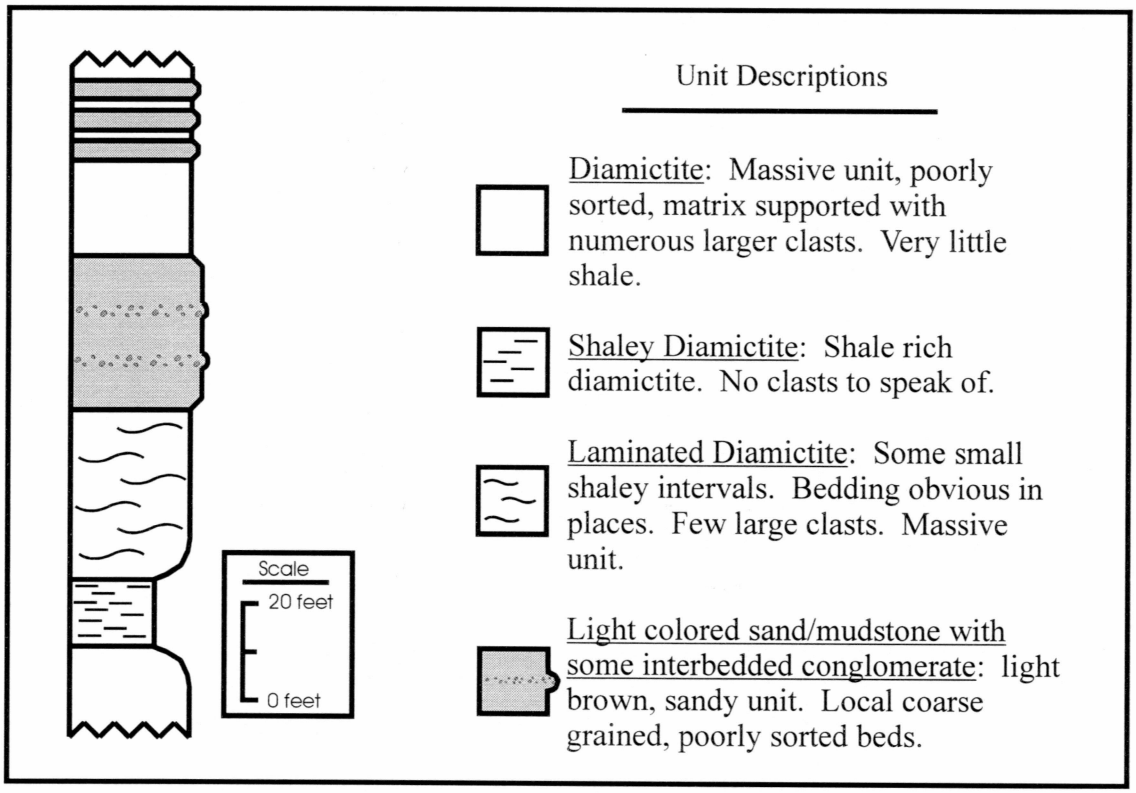

Figure 18, **Local Icy Bay stratigraphy**: Section I measured at the accessible fault-tip region of the Yakataga anticline. Unit thicknesses and lithologies change laterally over short distances due to the numerous channels dissecting the stratigraphy.

Figure 19a, **Soft sediment deformation**: This picture was taken just south of, and stratigraphically above, the ramp tip, in horizontal, structurally undeformed sediments. Black lines trace out bedding and illustrate the impressive soft-sediment deformation that was common throughout the area.

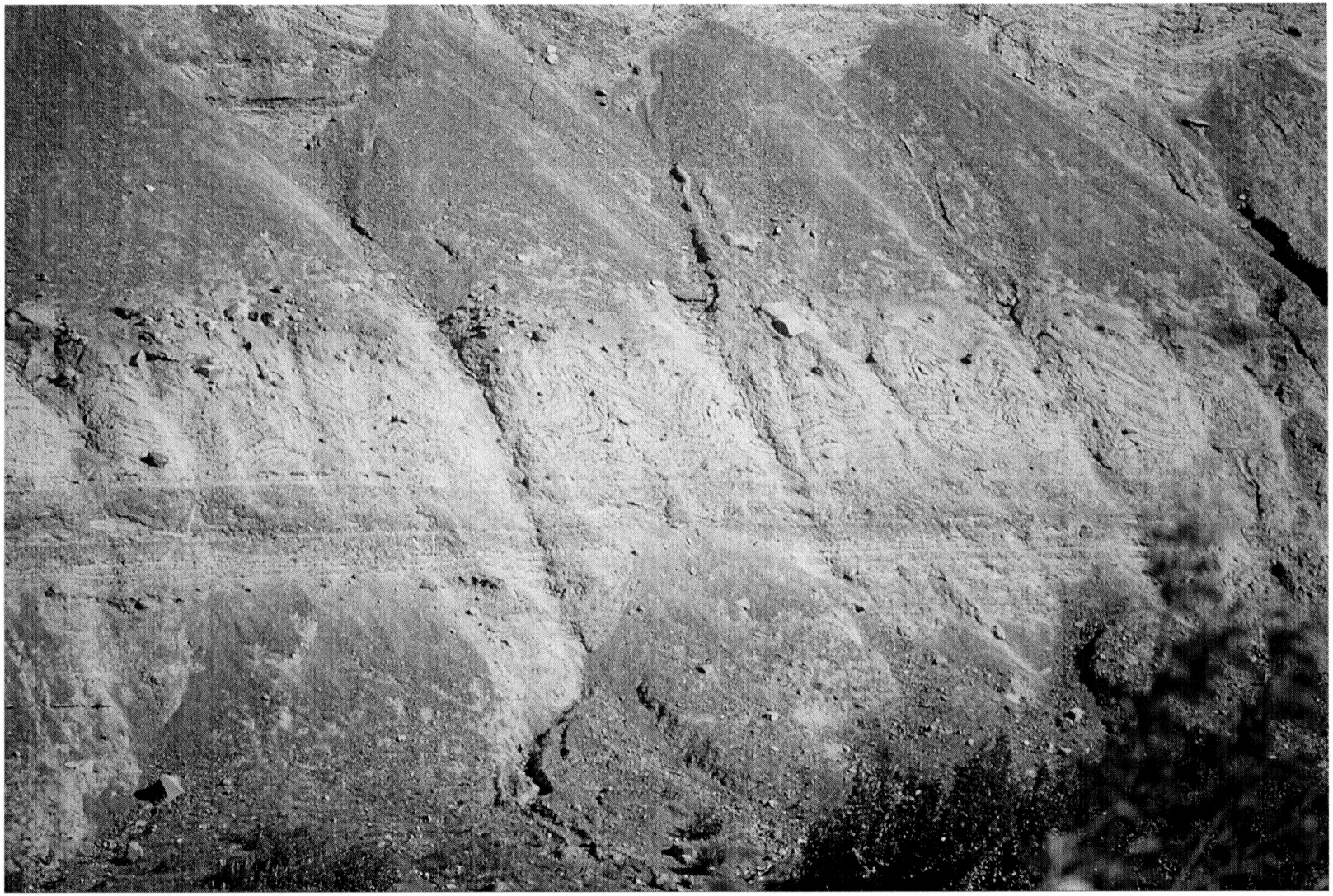

Figure 19b, **Soft sediment deformation**: Uninterpreted photo of soft-sediment deformation..

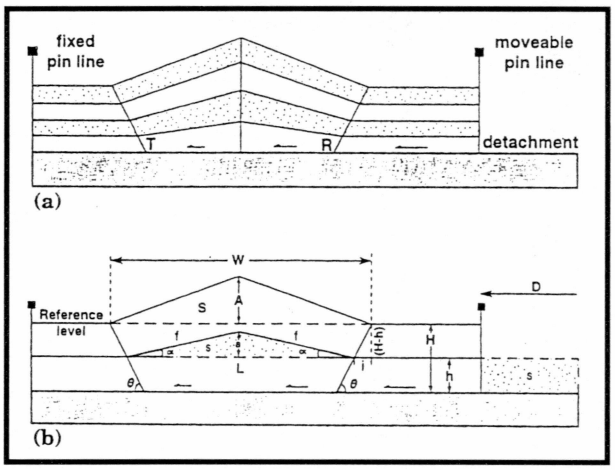

Figure 20, **Epard and Groshong detachment fold model**: T = tip of the fault, R = rear fold hinge. (a) Position of the pin lines, axial surfaces and detachment. (b) Notation: D = displacement; H = height of reference level above the detachment; A = amplitude of the fold with respect to level H; W = width of the fold at level H; S = excess area (of amplitude A produced by displacement D above level H); h = height of any level above the detachment; a = amplitude of the fold for level h; L = width of the fold at level h; s = excess area produced by displacement D above level h; f = length of the limb. Their model, in order to area balance, requires $s = Dh$. The above example is for the simplest case of a triangular, symmetric detachment fold, but the model works for other fold geometries as well. From Epard and Groshong (1995).

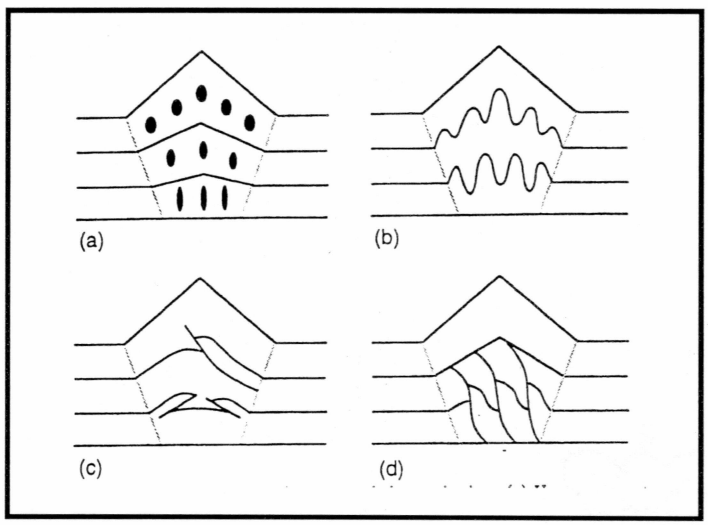

Figure 21, **Strain accommodation mechanisms**: Schematic diagrams of detachment folds with alternative strain accommodation mechanisms. (a) Penetrative strain. (b) Second-order folding. (c) Second-order conjugate faulting. (d) Duplex in fold core. From Epard and Groshong (1995).

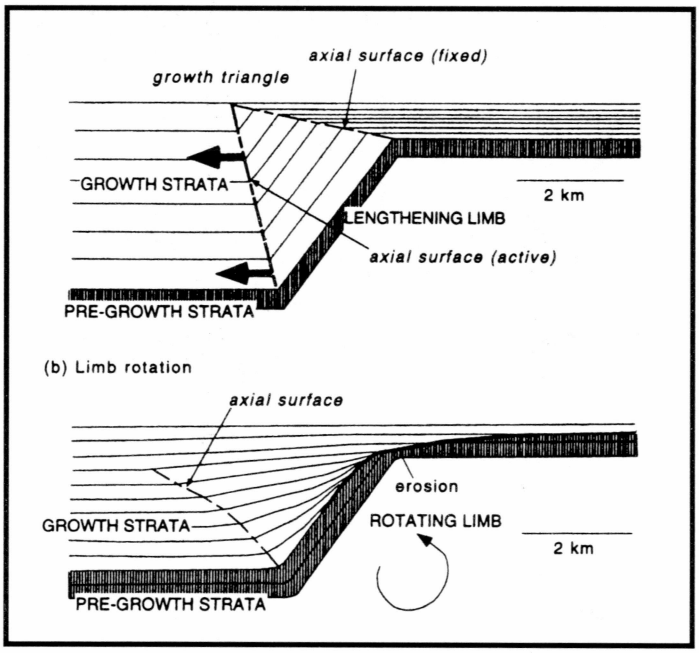

Figure 22, **Growth strata geometries**: Diagram showing the expected geometries of growth strata in a monoclinal fold with a) a fixed limb dip, and b) a rotating limb. From Ford and others (1997).

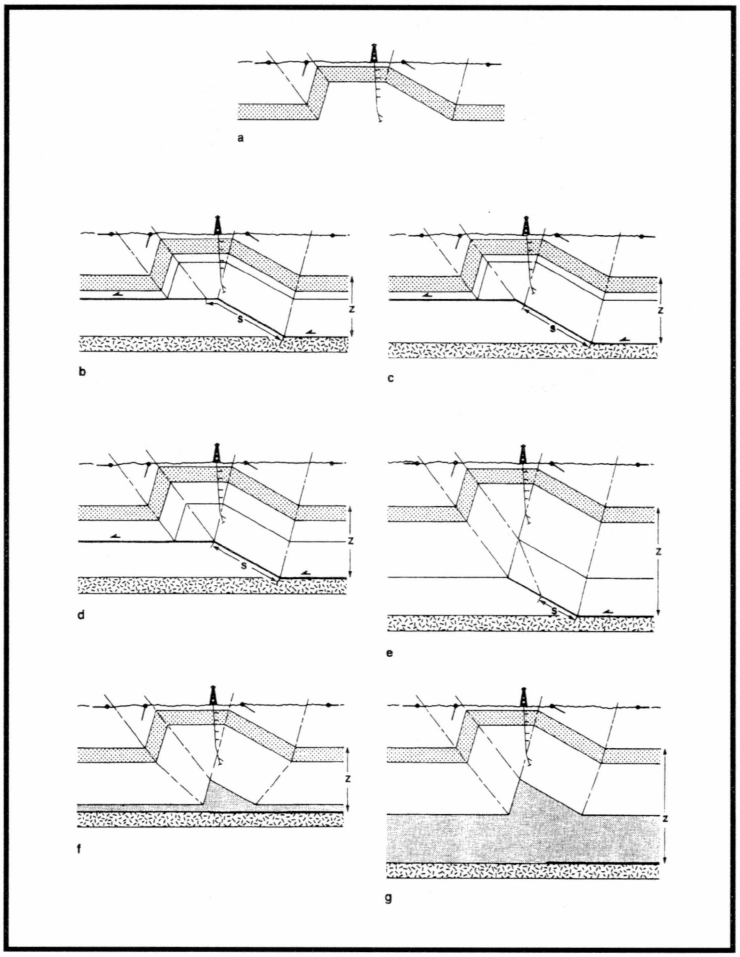

Figure 23, **Fold model impications**: Series of drawings showing that several thrust-related fold models can be fit to a single geometry of the upper part of the fold. (a) shows the near-surface fold geometry. (b-d) show variations on fault-bend folds that fit the data. (e) shows a fault-propagation fold with the maximum depth to detachment and the minimum shortening. (f -g) both show detachment fold models with different depths to detachment. The fold geometry is consistent with any of the above interpretations. From Mitra (1990).

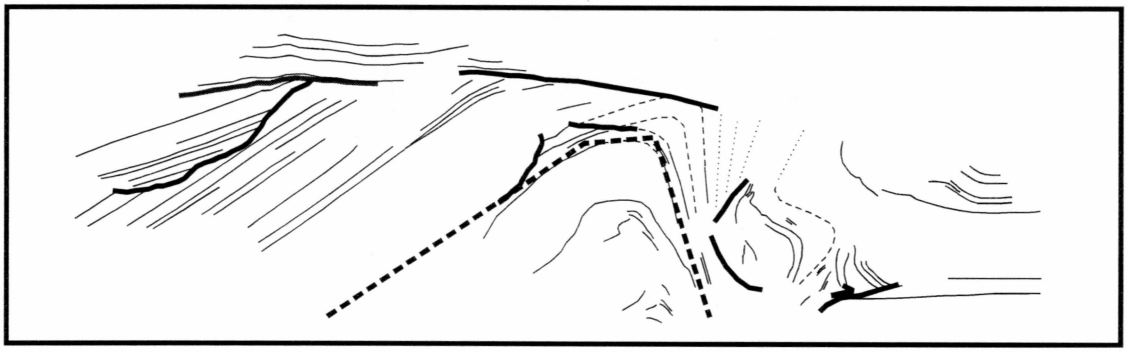

Figure 24, **Initial detachment fold geometry**: Inferred original geometry of the lower-most bed in the detachment fold (thick, short-dashed line) overlain on the cross section of the Yakataga anticline. Thick black lines are unconformities, thin black lines are bedding planes (dashed where inferred).

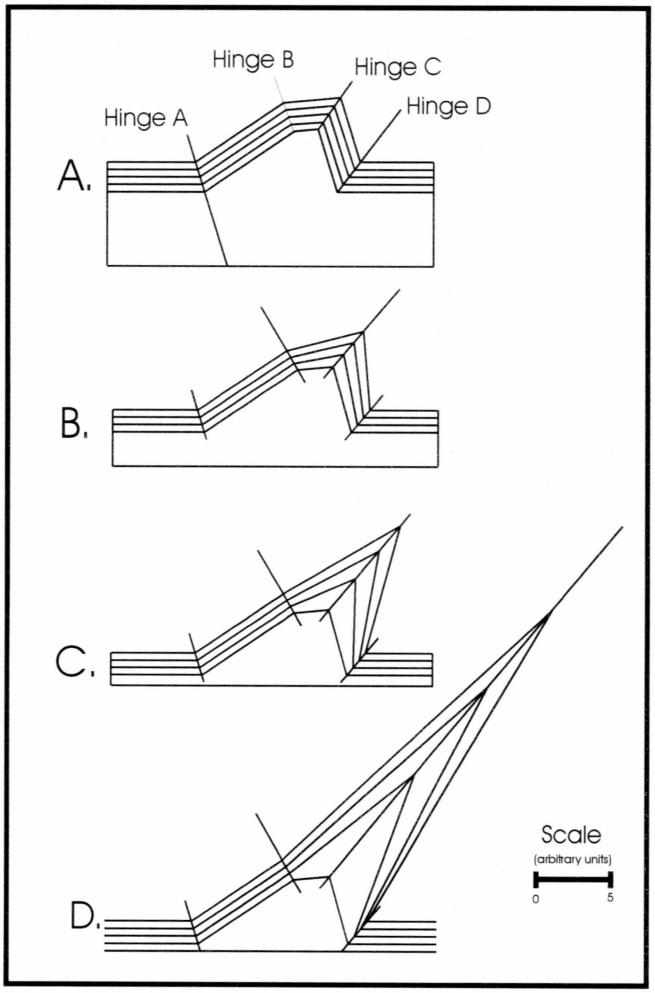

Figure 25, **Depth to detachment determination**: Diagrams showing the effects of altering the depth to detachment on higher beds given a constant geometry of the lowest marker bed. Folds built according to Epard and Groshong (1995). All measurements are in arbitrary units.

A) Depth to detachment of 5.0, with a shortening of 4.33.

B) Depth to detachment of 3.5, with a shortening of 7.6.

C) Depth to detachment of 1.5, with a shortening of 17.73.

D) Depth to detachment of 0.5, with a shortening of 53.2.

As the depth to detachment decreases, the fold starts to amplify along the thickening hinge. It is not illustrated here, but with a depth to detachment of 5.28, the fold geometry is perfectly parallel. The upper beds start to collapse if depth to detachment is increased beyond this point, as determined through other experiments not shown here. All depths to detachment are measured from the lowermost bed.

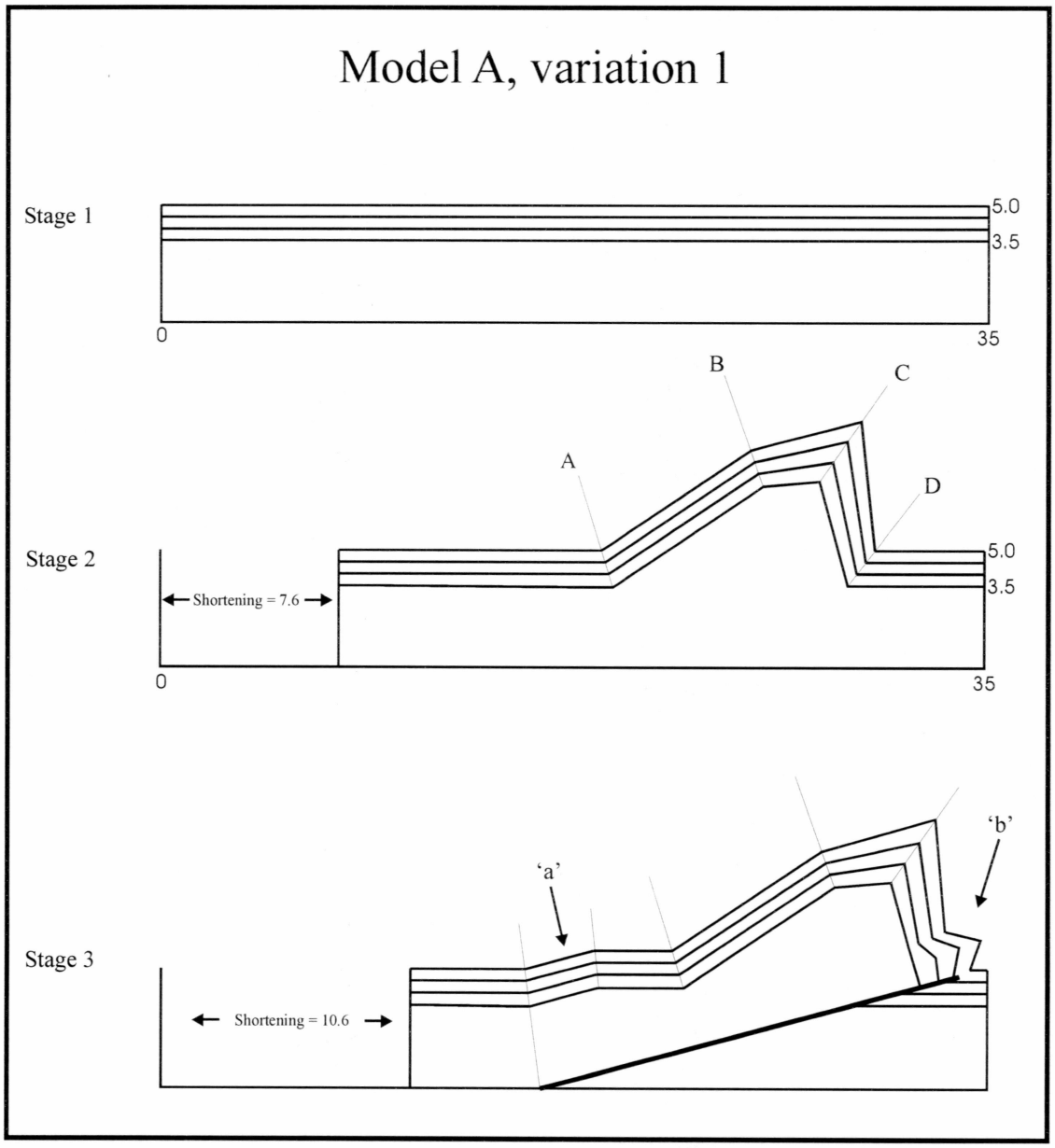

Figure 26, **Model A, variation 1**: Variation 1 on a detachment fold with later superimposed fault-propagation folding. The model has an initial depth to detachment of 3.5 units from the lower-most marker bed. The fold forms from original horizontal beds (stage 1) as a detachment fold according to the Epard and Groshong (1995) model. The fold reaches the geometry seen in stage 2 before a ramp starts to cut up section at a dip of 15 degrees. The ramp is seen as a thick, black line in stage 3. As shortening continues, fault-propagation folding overprints the original detachment fold geometry, causing two significant features: 'a,' a backlimb kink; and 'b,' a secondary fold in the forelimb.

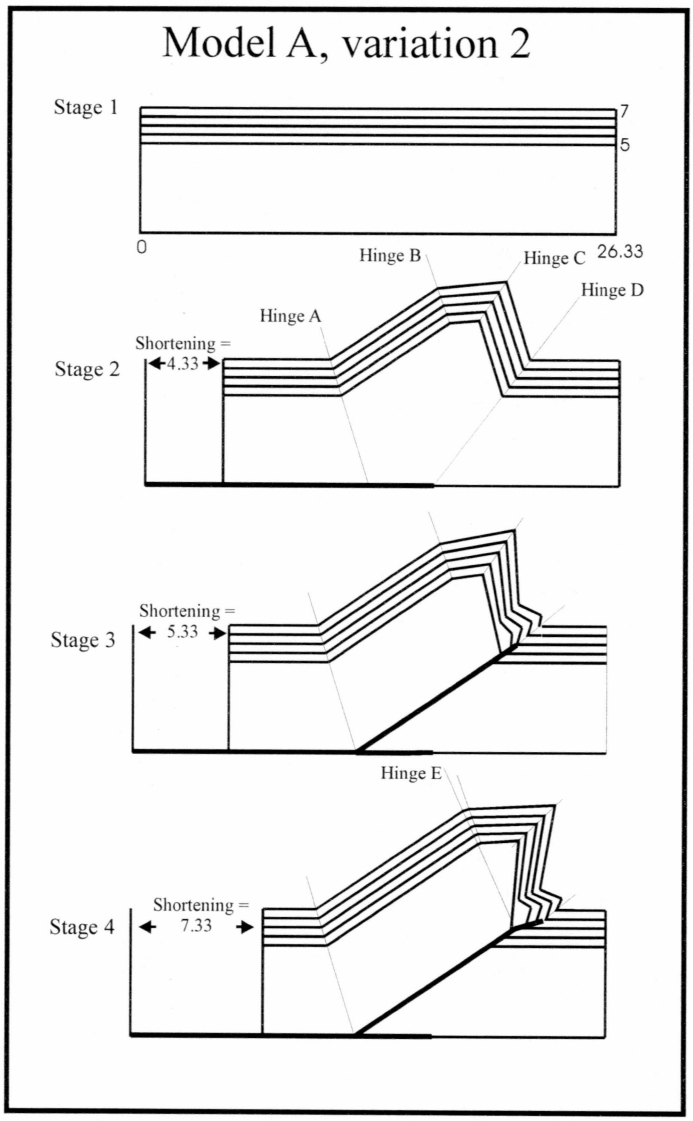

Figure 27, **Model A, variation 2**: Variation 2 on a detachment fold with later superimposed fault-propagation folding. Variation 2 has an initial depth to detachment of 5 units from the lowermost marker bed. The model starts as originally horizontal beds (stage 1) that are deformed initially as a detachment fold according to the Epard and Groshong (1995) model. The final detachment fold geometry is shown in stage 2. At this point, a ramp starts cutting up section and a fault-propagation fold starts to form as the ramp propagates from a point near the lowermost marker bed. To this point, the fold forms similarly to variation 1, with all differences due to the difference in initial detachment depth. In stage 4, the ramp changes angle, and another hinge (E) is formed, which serves to tilt the forward part of the fold 19 degrees clockwise. This tilt is accommodated by non-parallel folding in the forelimb in which marker beds have been tilted forward as passive markers.

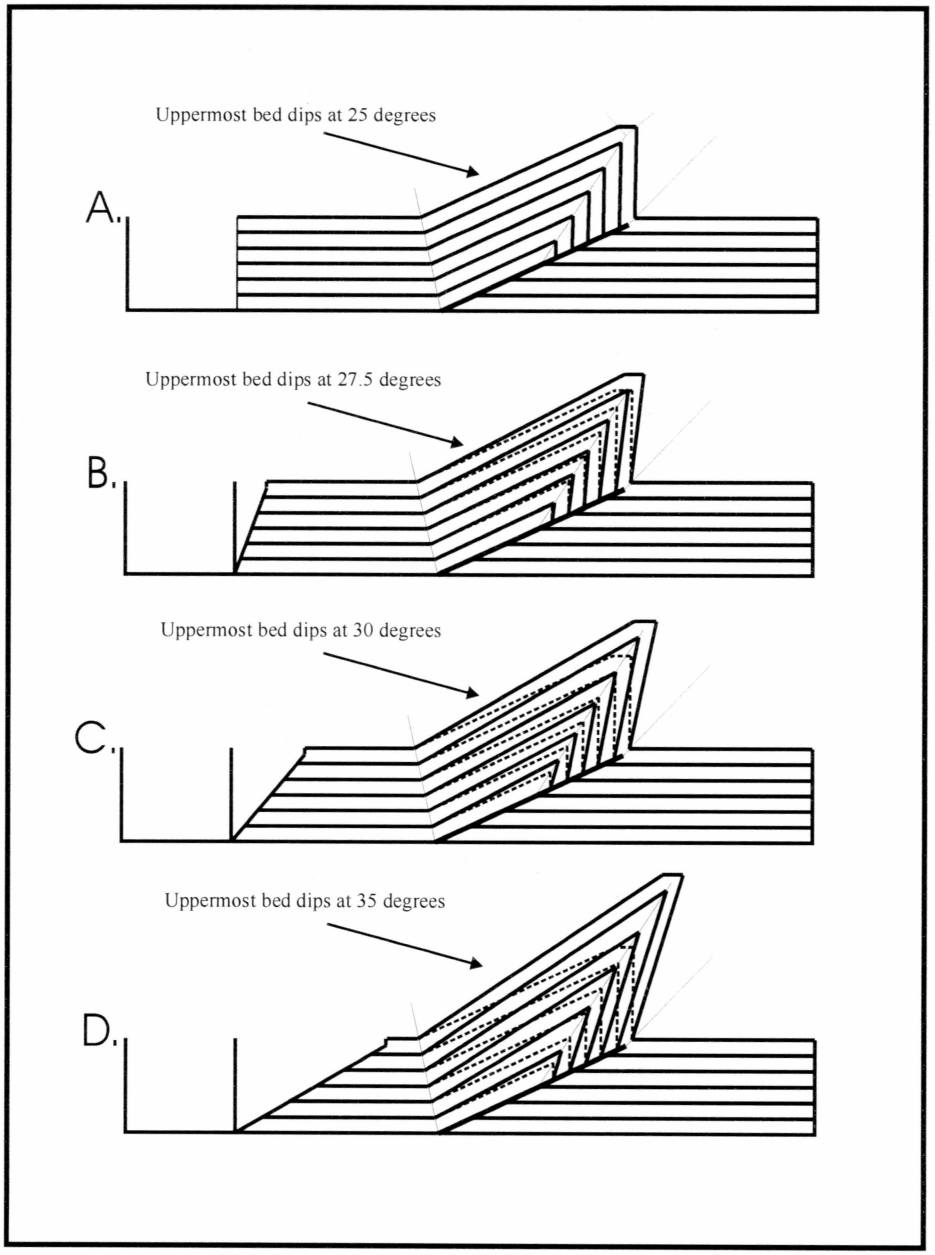

Figure 28, **Shear determination**: Series of diagrams showing the limb rotation that results from applying varying amounts of shear to a simple fault-propagation fold. Geometry from 'A' included in 'B' through 'D' as dashed lines for a basis of comparison to the fold without any shear added. A) Original fault-propagation fold with no shear. B) 20 degrees of shear added, resulting in a maximum of 2.5 degrees of rotation. C) 40 degrees of shear added, resulting in a maximum of 5 degrees of rotation. D) 60 degrees of shear added, resulting in a maximum of 10 degrees of rotation. With ramp angle of 25 degrees, this makes the steepest beds in the backlimb reach a dip of 35 degrees, which is in good agreement with the natural fold.

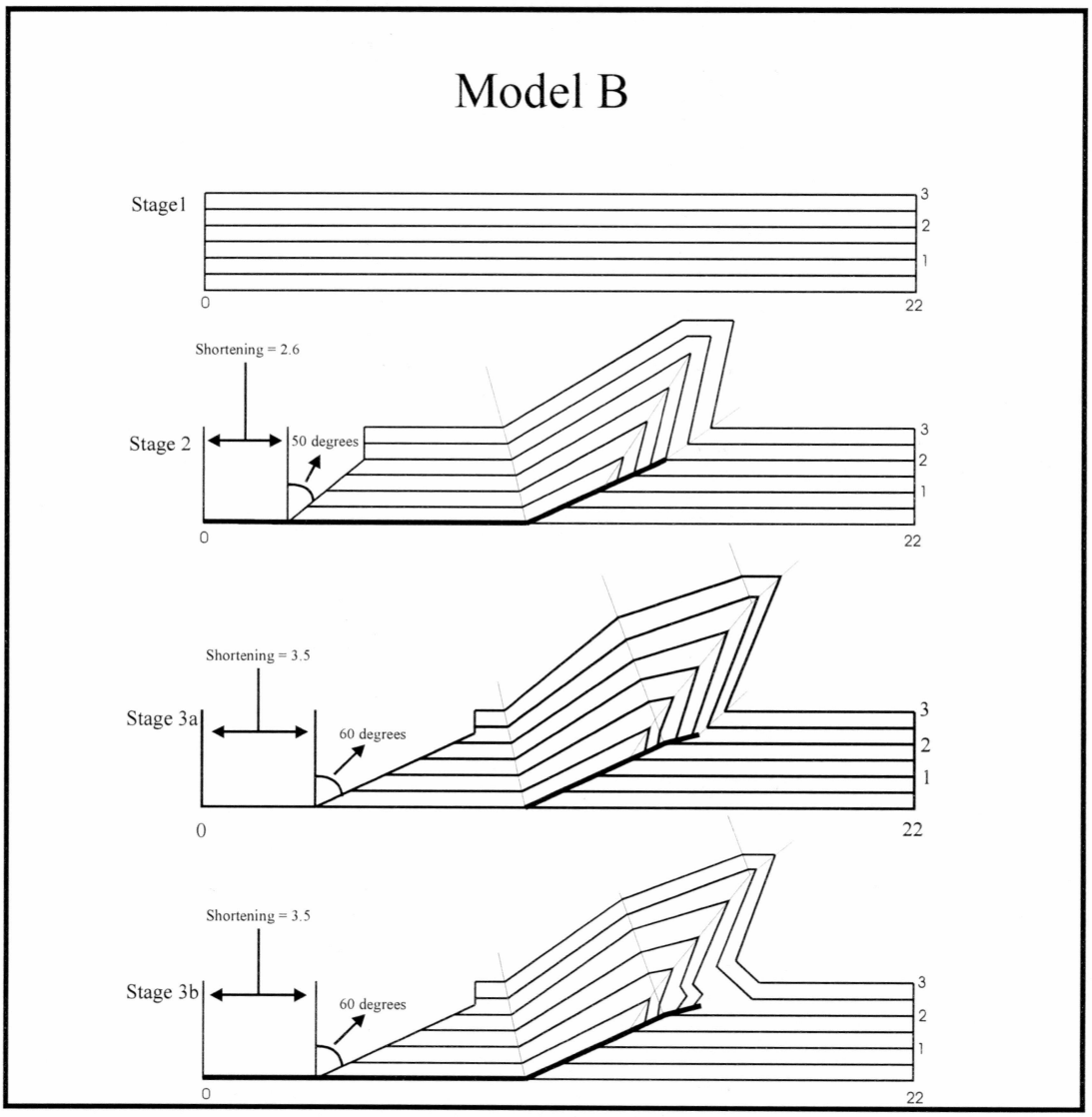

Figure 29, **Model B**: Progressive development of Model B, a rotating-limb fault-propagation fold. Stage 1) The fold starts with initially horizontal beds. Stage 2) The fold grows as a fault-propagation fold, with the addition of a shear gradient. The shear is accommodated by thickening in both the forelimb and the backlimb, resulting in hinge thickening and rotation of the beds. It is not obvious in the diagram, but the rotation causes a fanning of the beds. In stage 2, the lowermost bed above the ramp dips at 28 degrees while the uppermost bed dips at 31 degrees. At this stage, the ramp propagates at a 25 degree angle. Stage 3a) The ramp changes angle up-section to 15 degrees. This spawns a new hinge, which serves to tilt the forelimb forward. Stage 3b) This stage was included to show the possibility of a secondary fold forming in the forelimb. No aspect of the model required this feature, but since it is present in the natural fold, I included it here. I hypothesize that it formed due to oversteepening of the forelimb and gravitational collapse of material into the secondary fold.

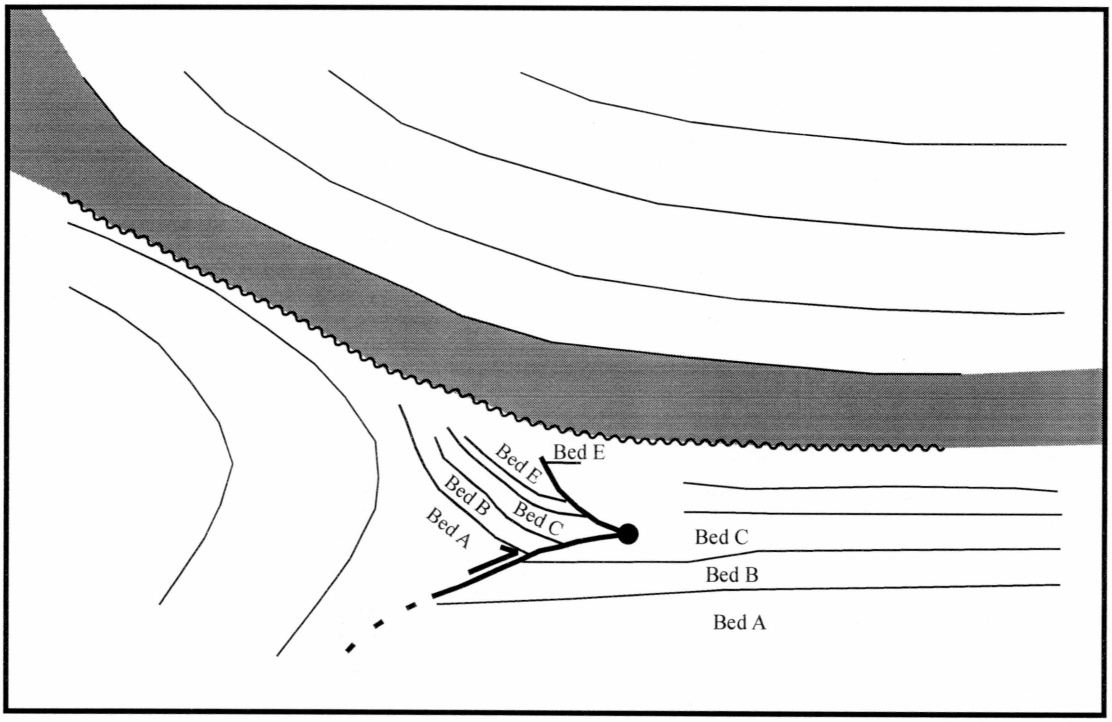

Figure 30, **Unconformity interpretation**: A line sketch of the area around the fault tip (Figure 15) to illustrate the space problems in the lower part of the anticlinal forelimb. The area highlighted in gray shows the lowermost bed unaffected by the secondary fold. More steeply dipping beds above the upper part of the ramp are truncated below this bed. This proposed unconformity would fit well with the interpreted unconformity in the forelimb (Figures 10, 12, and 13).

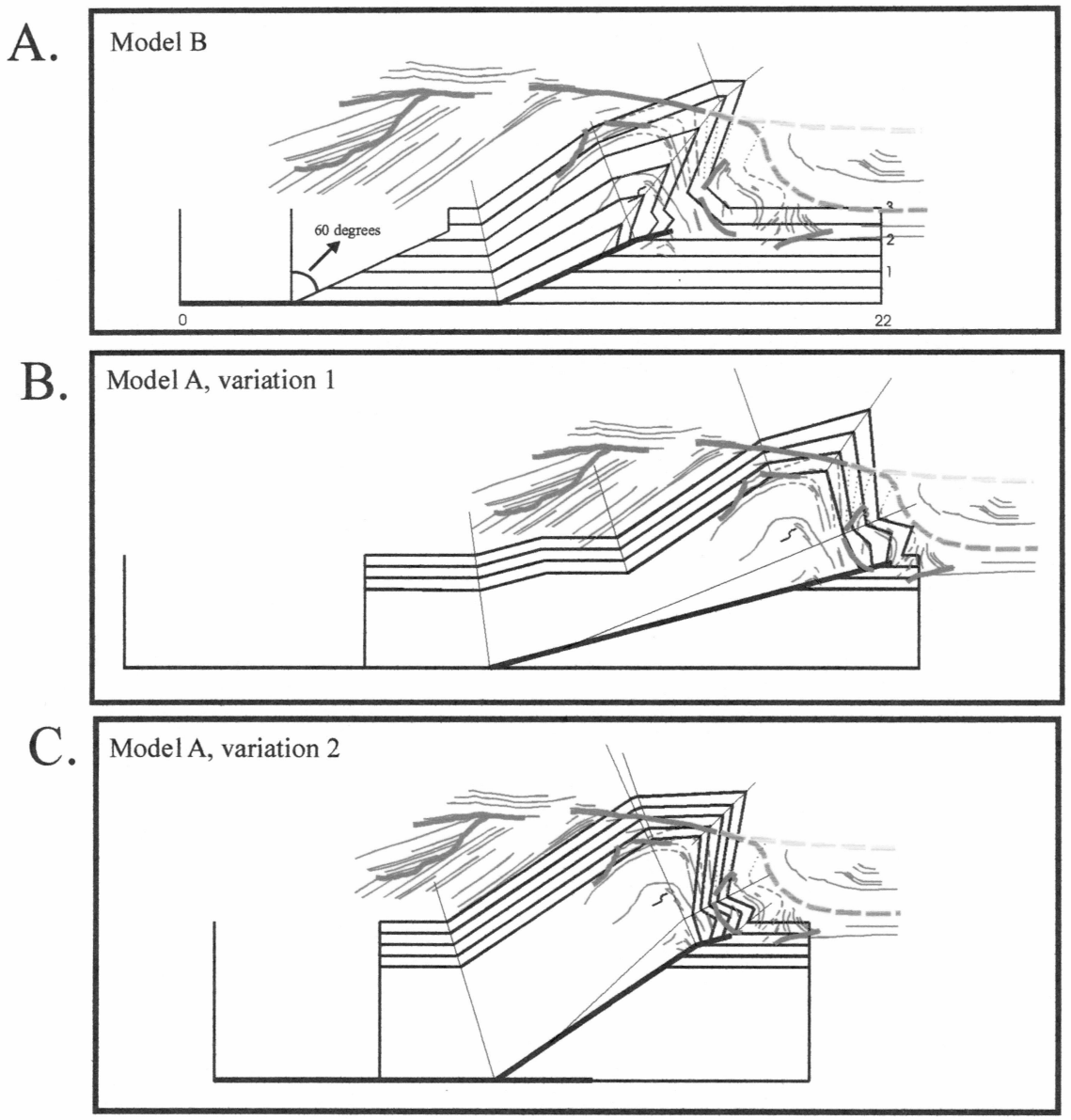

Figure 31, **Model Comparisons**: Caption follows.

Figure 31, **Model Comparisons**: Cross section of the natural fold, shown in red, superimposed on cross sections of Model B (Figure 29, stage 3b), Model A, variation 1 (Figure 26, stage 3), and Model A, variation 2 (Figure 27, stage 4). Two possible extensions of the highest unconformity in the natural fold are shown in blue and green.

A) Model B: This model results in a geometry similar to that of the natural fold, but when the cross section of the natural fold is superimposed on the model, there is actually little agreement. The location of the fault ramp relative to the fold core is very different, and the forelimb dips do not fan as seen in the Yakataga anticline. The backlimb dips do fan, however, which is not seen in the natural fold.

B) Model A, variation 1: The location of the fold core relative to the ramp again does not match, but it is a much closer fit than seen in either of the other two possibilities shown. If this model is assumed to be correct, the kink in the backlimb is apparently not completely buried and should be visible. The forelimb does not steepen as much as in the natural fold either.

C) Model A, variation 2: The location of the ramp relative to the fold core is not in as good agreement as in model A, variation 1, but it is a better fit than in Model B. The forelimb dips steeply enough, but does not fan as the natural fold apparently does. If this model is assumed to be correct, then beds visible in the backlimb should flatten north of the hindward syncline hinge, but this is not seen in the natural fold.

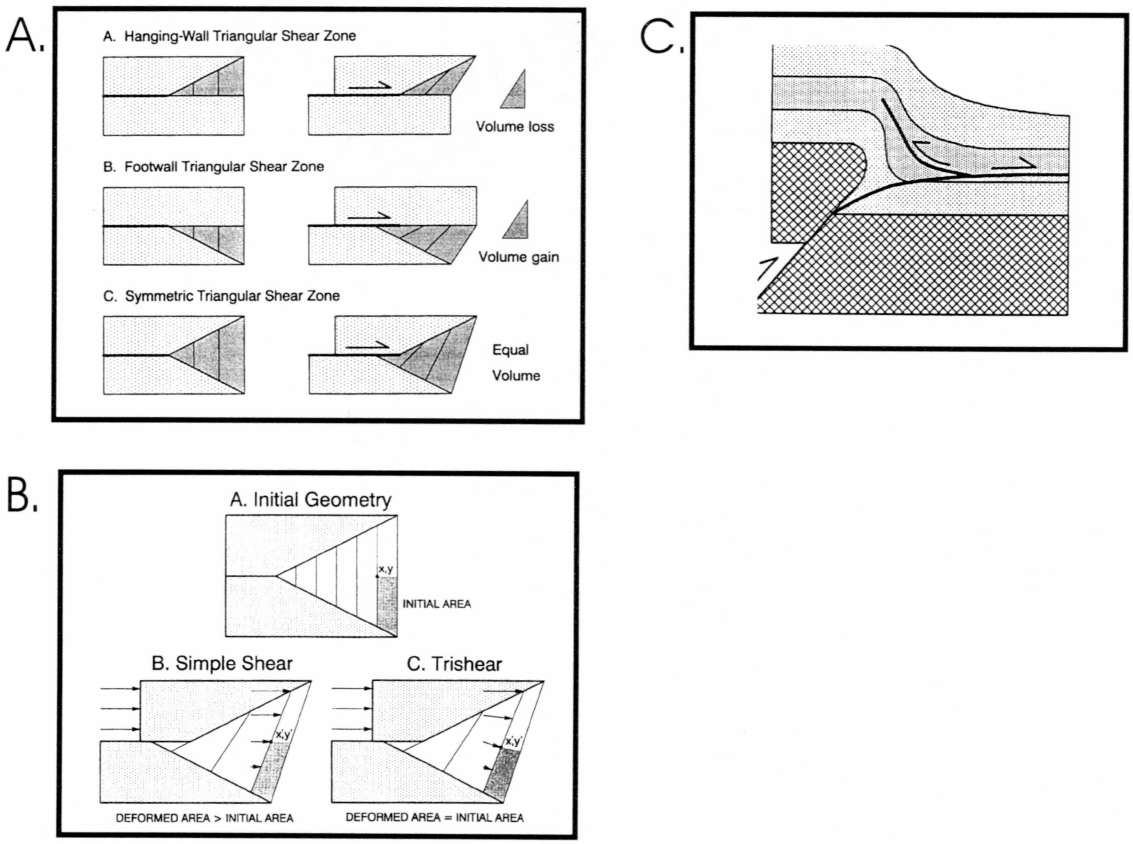

Figure 32, **Trishear model**: Erslev's tri-shear model provides an alternative kinematic model for fault-propagation folds by distributing shear in a triangular shear zone focused from the fault tip. Using the trishear fold model can replicate a wide range of fold shapes, but in all cases the back-limb of the fold is still contolled by the ramp dip. A) "Geometric end members of triangular shear zone folding." B) "Simple shear and trishear approximations of homogeneous shear in triangular shear zones." C) One example presented by Erslev (1991) of a fault-propagation fold with homogeneous, footwall-fixed trishear in front of the thrust fault. This example approximates many features of the Yakataga anticline. All figures from Erslev, 1991.

Appendix: Air photos used during interpretations of the Yahtse anticline.

Appendix continued.